The Sun's variable radiation and its relevance for Earth

Article *in* Annual Review of Astronomy and Astrophysics · September 1997

DOI: 10.1146/annurev.astro.35.1.33

CITATIONS
226

READS
3,125

1 author:

Judith Lean
United States Naval Research Laboratory
131 PUBLICATIONS **15,929** CITATIONS

SEE PROFILE

Annu. Rev. Astron. Astrophys. 1997. 35:33–67

THE SUN'S VARIABLE RADIATION AND ITS RELEVANCE FOR EARTH[1]

Judith Lean
EO Hulburt Center for Space Research, Naval Research Laboratory,
Washington, DC 20375; e-mail: lean@demeter.nrl.navy.mil

KEY WORDS: solar variability, climate change, ozone, space weather, upper atmosphere, ionosphere

ABSTRACT

To what extent are changes in the Earth's global environment linked with fluctuations in its primary energy source, the radiation from a variable star, the Sun? A firm scientific basis for policy making with regard to anthropogenic greenhouse warming of climate and chlorofluorocarbon depletion of ozone requires a reliable answer to this question. Reduction of the vulnerability of spacecraft operations and communications to space weather necessitates knowledge of solar induced variability in Earth's upper atmosphere. Toward these goals, solar radiation monitoring and studies of solar variability mechanisms facilitate an understanding of the sources and amplitudes of the Sun's changing radiation. Interdisciplinary studies that link these changes with a wide array of terrestrial phenomena over the longer time scales of global change and the shorter time scales of space weather address the relevance of solar radiation variability for Earth. However, although numerous associations are apparent between solar and terrestrial fluctuations, full comprehension of the physical mechanisms responsible for the many facets of radiative Sun-Earth coupling remains to be accomplished.

1. INTRODUCTION

Solar radiation is an unfailing source of energy for the Earth. Without visible and infrared (IR) radiation from the Sun, Earth's surface temperature would be too cold to support life. Nor would there be energy to fuel photosynthesis or power the circulations of the lower atmosphere and oceans that profoundly

influence living organisms. Lacking solar ultraviolet (UV) radiative inputs, Earth's middle atmosphere would be devoid of ozone and its upper atmosphere cold and unionized. Living things would be exposed to damaging high-energy solar photons. Society would lack the many benefits of Earth-orbiting spacecraft and global communication. For these reasons monitoring, understanding, and predicting the Sun's radiation variability and its terrestrial impacts is a component of the US Global Change Research Program (Committee on Earth Sciences 1989), the National Space Weather Program (1995), NASA's Mission to Planet Earth (Hartmann et al 1993), Space Environment Effects (NASA 1994) and Sun-Earth Connections Programs, and one of five key current topics in space physics research (National Research Council 1995).

Emergent from the Sun's atmosphere at wavelengths spanning the entire electromagnetic spectrum from X rays to radio waves, solar radiation achieves maximum flux levels at the visible wavelengths that are essential for photosynthesis and human processes. After nearly five billion years of evolution, the Sun has been such a reliable, steadily emitting star that its total radiative energy at the Earth is known historically as the solar "constant," a quantity whose value at the mean distance of the Earth from the Sun is measured to be $S = 1366$ W/m^2 (with an uncertainty of ± 3 W/m^2).

Although more than a century of ground-based monitoring failed to determine whether the Sun's total radiative energy was truly constant (Hoyt 1979), fluctuations in other solar phenomena—especially the changing patterns of features on the Sun's surface—have long intrigued both solar and terrestrial observers. Dark sunspots appear to move across the face of the Sun as it rotates once every 27 days. Sunspots exhibit, as well, a pronounced quasiregular 11-year cycle in their number (discovered by Schwabe in 1843) that has been particularly strong in recent decades. Purported correlations of solar variability and climate have been reported for more than a century (Meadows 1975, Eddy 1976), then abandoned under statistical scrutiny and for lack of adequate physical mechanisms (Pittock 1978), only to reemerge (Reid 1991, Friis-Christensen & Lassen 1991) for renewed scrutiny (Kelly & Wigley 1992, Schlesinger & Ramankutty 1992, Reid 1995).

Discovery of the ozone layer in the 1920s, and recognition of the critical role of the Sun's UV radiation in its formation, initiated curiosity about the likely impact of solar variability on Earth's middle atmosphere (from 15–50 km above the surface). But attempts to identify the causes of long-term ozone and middle atmosphere changes evident in ground-based monitoring were inconclusive (Angell & Korshover 1973). Apparent correlations of ozone, zonal winds, and temperature with solar variability were detected (Paetzold 1973, Nastrom & Belmont 1978, Quiroz 1979), but the amplitudes of UV radiation variability were too poorly known to facilitate definitive simulations (Penner &

Chang 1979). And, like weather and climate near the surface, Earth's middle atmosphere experiences large seasonal and biannual variability that obscures decadal trends.

Robust associations did, however, emerge between solar variability and the behavior of neutral and ion densities in the Earth's upper atmosphere (more than 100 km above the surface). Radio wave propagation via the ionosphere (Ellison 1969) and the orbits of artificial satellites (Jacchia 1963) exhibited strong associations with the Sun's 11-year cycle. Rocket-based solar observations made above the Earth's atmosphere detected significant levels of extreme ultraviolet (EUV) radiation, and variations of these emissions (Hinteregger 1970) offered a physical mechanism for the observed relationships (Nicolet & Swider 1963, Roble 1976, Roble & Emery 1983).

Solar monitoring during the past few decades now affords a broader perspective of solar variability and its mechanisms. The familiar 11-year sunspot cycle is but one manifestation of our intrinsically inconstant Sun. Essentially all solar phenomena exhibit 11-year cycles, including radiative output (White 1977), particle and plasma emissions, interior oscillations, and perhaps even fundamental processes in the Sun's nuclear burning core (Cox et al 1991, Sonett et al 1991). Solar variability is also evident on other time scales. Oscillations below the Sun's visible surface and flaring of its outer atmosphere modulate the Sun's radiation on time scales of minutes to hours (Hudson 1987, Donnelly 1976). Proxies of solar activity archived by ^{10}Be and ^{14}C cosmogenic isotopes in ice cores and tree rings, respectively, indicate variability modes with periods near 87, 206, 512, and 2400 years (Stuiver & Braziunas 1993, Beer et al 1988).

Since the first curiosity-driven discoveries of solar terrestrial linkages, a more urgent imperative has emerged to quantify the relevance for Earth of the Sun's variable radiation (National Research Council 1994). Changes in our terrestrial environment can have extensive consequences for habitability, biodiversity, and technological infrastructures. Requisite for policy making to regulate greenhouse gas and chlorofluorocarbon (CFC) emissions is a firm assessment of the extent to which observed climate and ozone changes are of anthropogenic versus natural origin. Efficient utilization of the space environment requires operational specification of how changing neutral and ion densities impact the performances, lifetimes, and reentries of Earth orbiting spacecraft and the efficiency of radio frequency communications, with adequate predictive capability to support national needs.

2. SPECTRUM OF SOLAR RADIATION

A nuclear burning core generates the Sun's energy. Radiative processes transport this energy outward from 0.3 to 0.7 solar radii, and convective motions in

the outer third of the Sun's interior deliver it to the visible solar surface. Above the Sun's surface—defined as that layer of the Sun from which radiation at 500 nm emerges at unit optical depth—a strongly ionized plasma extends for thousands of kilometers into space. This plasma comprises the solar atmosphere, the source of the Sun's radiation (for details see Foukal 1990, Cox et al 1991).

Temperature and composition at the Sun's surface and within the solar atmosphere (shown in Figure 1*a*) dictate the spectral structure of emitted radiation. In a solid angle subtended at the Earth at a distance of 1 AU, the Sun's radiant energy produces an irradiance spectrum (shown in Figure 1*b*) that has maximum levels near 500 nm and decreases to more than six orders of magnitude less in the X-ray and radio spectral regions. Some 48% of the Sun's total (spectrally integrated) irradiance of 1366 W/m^2 is at visible and near-IR

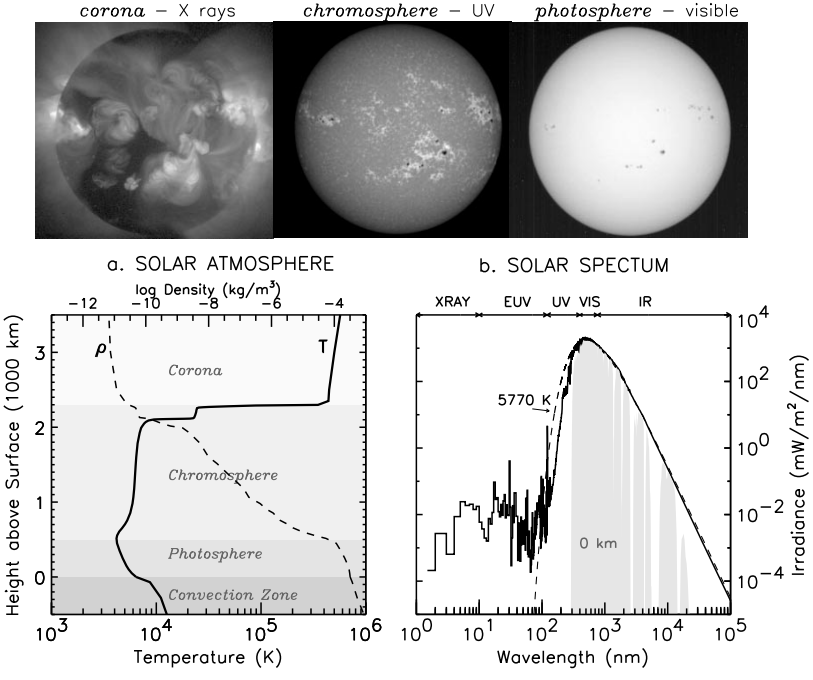

Figure 1 Conditions of temperature and density at the Sun's surface and in its atmosphere (*a*) determine the solar irradiance spectrum (*b*). Magnetic fields distributed throughout the solar atmosphere alter the mean temperature (T) and density (ρ) profiles in (*a*), generating inhomogeneities in the distribution of radiation emitted from the solar disk, shown on January 10, 1992, for X-ray emission from the corona (*left image*), Ca II K emission from the chromosphere (*middle image*, made by the Big Bear Solar Observatory) and visible light from the photosphere (*right image*). Evolution of these surface inhomogeneities in turn modulates the irradiance spectrum.

wavelengths from 400–800 nm and emerges from the lowest layer of the solar atmosphere—the photosphere (Figure 1*a*)—with a spectral shape similar to the curve of black-body emission at 5770 K (Figure 1*b*).

Numerous spectral features punctuate the smooth continuum of photospheric radiation. Absorption and emission processes of ionized constituents in the Sun's atmosphere produce spectral features with widths from a few tenths to more than one angstrom. The least absorption by the solar atmosphere of the underlying photospheric continuum emission occurs in the vicinity of 1.6 microns (μ) (1600 nm), and this radiation thus emerges from the deepest observable layer of the Sun. The spectrum at both longer and shorter wavelengths originates at greater heights because the opacity of the solar atmosphere is larger than at 1.6 μ (Vernazza et al 1976). In the UV spectrum (120–400 nm), absorption by many species—Al, Mg, Ca, O, Fe, H—depletes the underlying continuum radiation so much that the equivalent blackbody temperature of radiation near 160 nm is reduced from 5770 K to 4500 K. This temperature occurs at about 500 km above the Sun's visible surface and defines a minimum in the solar atmosphere temperature that delineates the upper boundary of the photosphere (Figure 1*a*). The spectrum from 75 μ to 300 μ also originates in the temperature minimum region as a result of increasing photospheric absorption at longer IR wavelengths.

Temperatures in the solar atmosphere rise slowly for another 1500 km above the temperature minimum (throughout the chromosphere), then increase dramatically in the transition region and corona. These hotter and higher atmospheric layers emit radiation shorter than 160 nm and longer than 300 μ, primarily by processes other than thermal radiation. Local conditions of density and temperature produce complex EUV (10–120 nm) and X-ray (0.1–10 nm) spectra that are dominated by line emission from multiply ionized species with fluxes well in excess of the photospheric black-body curve (Mariska 1992) (Figure 1).

3. SOLAR RADIATION VARIABILITY

Extensive evidence identifies the Sun as a variable star. Diverse solar parameters such as those in Figure 2 record this variability over wide ranging spectral and temporal scales. Like the sunspot number (Figure 2*e*), the total radiative output (Figure 2*c*) and the entire solar spectrum exhibit pronounced quasi-11-year and 27-day cycles, illustrated in Figure 2 for X rays (Figure 2*a*), UV radiation (Figure 2*b*), and radio waves (Figure 2*d*). Linking all aspects of solar radiation variability, as reviewed previously by Newkirk (1983) and Hudson (1988), is a common source, the magnetic activity of the Sun.

3.1 *Solar Activity*

Magnetic fields weave through the outer third of the Sun's interior—the convection zone (Figure 1*a*)—and penetrate the solar surface, extending outward

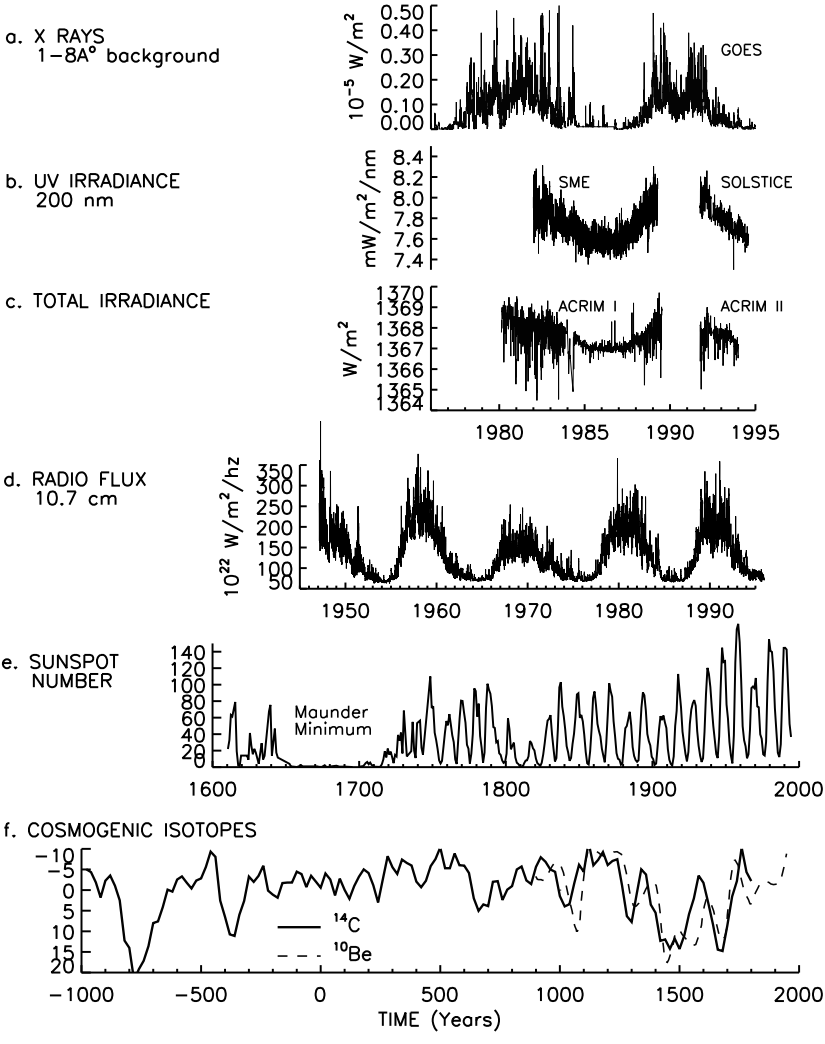

Figure 2 Variations occur in the Sun's radiation at wavelengths throughout the spectrum, seen in (*a*) the Geostationary Operational Environmental Satellite (GOES) 1–8 Å background flux, (*b*) the UV 200-nm irradiance measured by the Solar Mesosphere Explorer (SME) (Rottman 1988) and the Solar Stellar Irradiance Comparison Experiment (SOLSTICE) (Woods et al 1996), (*c*) the total irradiance measured by the Active Cavity Radiometer Irradiance Monitor (ACRIM) instruments on the Solar Maximum Mission (SMM) and the Upper Atmosphere Research Satellite (UARS) (Willson & Hudson 1991, Willson 1994), and (*d*) the 10.7-cm radio flux. These variations occur in concert with solar activity, whose long-term changes produce the variable sunspot record (Hoyt et al 1994) in (*e*) and affect as well the ^{14}C and ^{10}Be cosmogenic isotopes (*f*) in tree rings and ice cores, respectively (McHargue & Damon 1991, Stuiver & Braziunas 1993).

through the solar atmosphere. In the lower solar atmosphere, these field lines delineate patterns of granule and supergranule cells, defining the boundaries of the turbulent convective motions responsible for their transport to the surface. Higher in the solar atmosphere, the field lines fan out and either loop back to the surface to form large-scale emission structures, reconnect in situ, or continue outward into the solar wind and heliosphere. Magnetic fields nearer the Sun's equator rotate faster than those at higher heliocentric latitudes. This differential solar rotation stretches and shears the field lines, organizing patterns of magnetism that repeat with 11-year cycles. The combination of convective motions and differential rotation is thought to constitute a dynamo that drives solar activity (Nesme-Ribes et al 1996) and generates variability in a plethora of solar phenomena including radiative output. Because the polarity of the magnetic flux in each solar hemisphere reverses in successive 11-year cycles, the fundamental cycle length is actually 22 years.

In different solar atmosphere regimes, magnetic fields perpetrate distinctive features, which are displayed for the photosphere, chromosphere, and corona in Figure 1. In the photosphere (*far right image*), clumps of very strong magnetic fields—thousands of gauss—form sunspots that are darker and cooler than the surrounding photosphere because the magnetic fields somehow inhibit the upward flow of energy from the convection zone to the surface. Sunspots are compact in shape because gas pressure in the photosphere is large enough to balance the magnetic field strength. Less compact aggregates of field lines form faculae, which are slightly brighter than the surrounding photosphere and barely detectable in visible light images of the solar disk except near the limb (e.g. Foukal 1990).

Hundreds of kilometers above the Sun's surface the primary evidence of magnetic fields are bright regions called plages, which are evident in the image of the Sun's chromosphere in Figure 1 (*middle image*) made in the core of the singly ionized line at 393.4 nm—the Ca K Fraunhofer line. Plages correlate spatially with photospheric faculae and are sites of significant UV and EUV emission from the upper photosphere, chromosphere, and transition region (Dupree et al 1973, Cook et al 1980).

Magnetic fields in the solar corona are manifest in large-scale loops that confine extended volumes of bright emission, as seen in the soft X-ray (*far left*) image in Figure 1 made by the Soft X-ray Telescope (SXT) on the Yohkoh spacecraft (Tsuneta et al 1991, Acton 1996, Hara 1996). At coronal heights, the reduced pressure of the ionized solar atmosphere relative to magnetic pressure allows magnetic field lines to expand into large-scale complexes that can extend over much of the solar disk during times of high solar activity. Hot coronal loops generally overlay sites of the sunspots and plages (Noyes et al 1985), a correspondence evident in the images in Figure 1.

Also present on the Sun is a population of smaller-scale magnetic features that comprise newly emerging magnetic flux and remnants of decayed active regions (Harvey et al 1975, Tang et al 1984). Subsurface convective motions are thought to sweep these smaller magnetic features to the boundaries of granule and supergranule cells, where they trace out a network of bright emission over the entire surface of the Sun. This network disappears in radiation emitted at temperatures greater than 10^6 K (Reeves 1976), presumably subsumed in coronal loops of enhanced emission that dominate on large spatial scales. But in the chromosphere and photosphere, network emission is evident even during minima of 11-year activity cycles, possibly as a result of accumulated residual magnetism from past cycles, and is a source of variability in the contemporary Sun even when it is quietest (Gurman et al 1996).

3.2 *Sources of Solar Radiation Variability*

Magnetic phenomena are sources of significant solar radiation variability. Waxing and waning magnetic activity throughout the solar cycle produces changing sunspots, faculae, plages, and network that modify the Sun's net radiative output by altering temperature and density in the otherwise homogeneous solar atmosphere. Magnetic regions occur frequently when solar activity is high, typified by the January 1992 images in Figure 3, but they are sparse or absent during low activity epochs, such as in the February 11, 1994, image.

Solar activity does not influence the Sun's spectrum uniformly (Lean 1991). Figure 3 illustrates the changes in X-ray, UV, and total radiation concurrent with the evolution of solar magnetism from high activity in 1992 to lower levels in 1994. Dark sunspots and bright faculae act in opposition to modulate total irradiance and the spectrum at near-UV, visible, and IR wavelengths; the sunspot influence increases relative to the influence of faculae with increasing wavelength. In comparison, plage emission alone controls photospheric and chromospheric radiation variability in the UV and EUV spectrum at wavelengths less than about 300 nm. For example, while total irradiance in Figure 3*c* decreased 0.09% from January 16 to 31, 1992—because sunspot darkening exceeded facular brightening—the 200-nm irradiance actually increased by 5.5% (Figure 3*b*) in response to UV facular brightening alone. Coronal radiation (Figure 3*a*) generally tracks UV radiation because plasma emission is enhanced in magnetic field loops overlying large active regions that include both photospheric spots and chromospheric plages, but variations are significantly larger (145% from January 16 to 31, 1992).

Magnetic sources are apparently responsible for most, if not all, of the Sun's radiation fluctuations during the 27-day and 11-year cycles. Numerical simulations that combine the emission depletion in sunspots with enhancements in plages, faculae, and network replicate rotational modulation recorded in broad

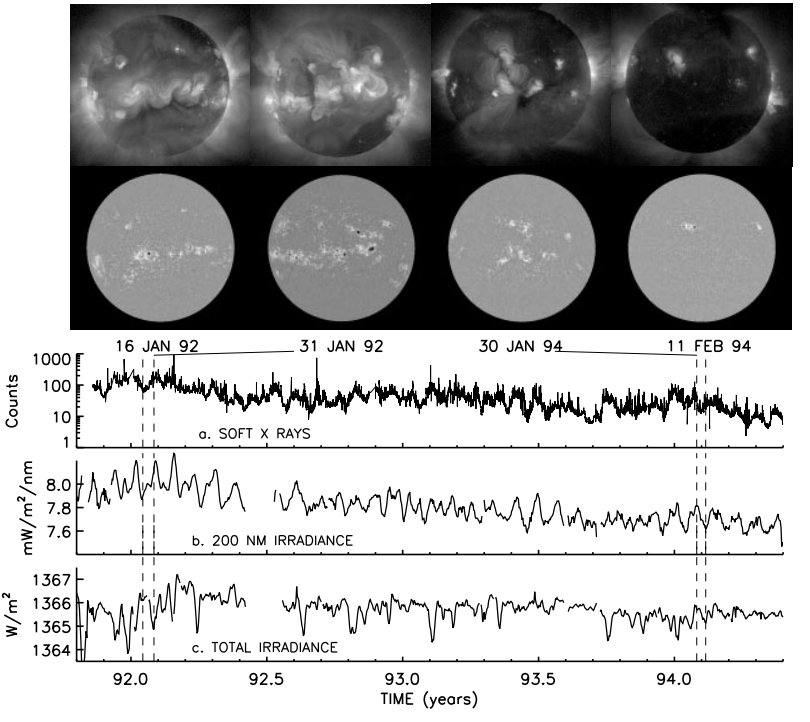

Figure 3 Evolution of solar activity from near maximum levels in 1992 to quieter conditions in 1994 alters the occurrence of bright and dark magnetic features on the Sun's disk, seen in coronal soft X-rays measured by the Soft X-ray Telescope on Yohkoh (*upper images*) and in chromospheric Ca II K images measured at the Big Bear Solar Observatory (*lower images*). The disk-integrated soft X-ray fluxes measured by Yohkoh in (*a*), the UV 200-nm irradiance measured by SOLSTICE in (*b*), and total irradiance measured by ACRIM on UARS in (*c*) track the overall decline in solar activity and also the Sun's 27-day rotation, which alters the distribution of active regions projected toward Earth.

UV and total irradiance bands shown in Figure 4 (Foukal & Lean 1990, Lean et al 1997a). Parameterizations that incorporate enhanced Ca K emission from full disk images (e.g. Figure 3) as a surrogate for radiation brightness successfully reproduce observed total, 200-nm, and C IV transition region irradiances during both the 27-day rotational modulation and the recent 11-year cycle decline (Lean et al 1997b, Warren et al 1996).

However, the brevity of solar monitoring—less than two 11-year cycles—combined with some sensitivity drifts in the monitors precludes unambiguous identification of all potential sources of radiation variability. The apparent

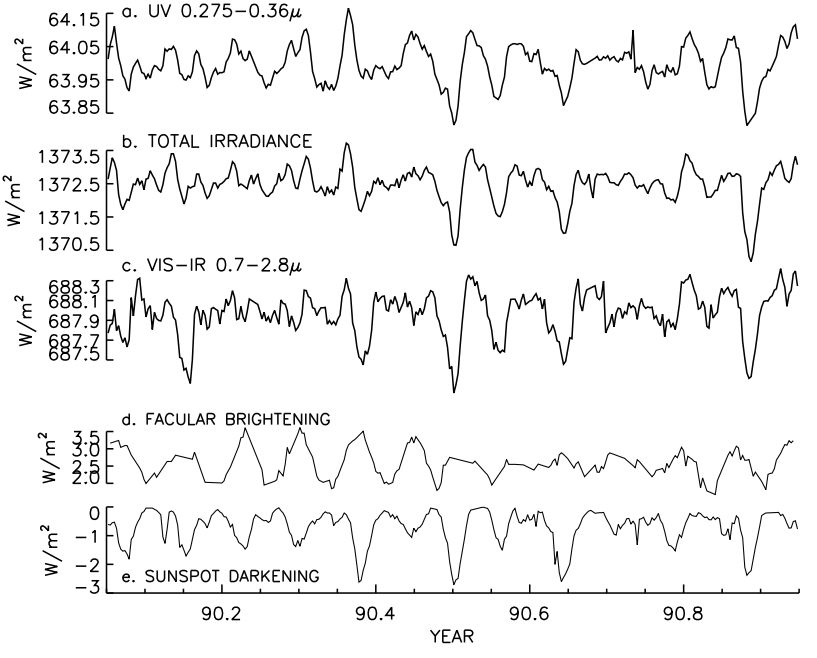

Figure 4 Variations occur in the Sun's radiation spectrum not only at the shorter UV and X-ray wavelengths but also in (*a*) the near UV and (*c*) visible to near IR radiation, as well as in (*b*) total radiation. Filter radiometers on the Nimbus 7 spacecraft (Kyle et al 1993) detected solar rotation modulation of these broad wavelength bands. Comparisons with proxies for facular brightening (*d*) and sunspot darkening (*e*) illustrate that the variations occur primarily because of the changing impacts of these magnetic features, whose opposing influences depend on wavelength.

inability of global brightness proxies to account fully for increases evident in some total irradiance measurements near activity maxima motivates speculation of a global brightness component—such as a few-degree change in solar surface temperature—in addition to magnetic sources (Willson & Hudson 1991, Kuhn & Libbrecht 1991, Fröhlich 1994). Nor are the variations in some strong emission lines—notably H I 121.6 nm—necessarily connected to magnetic sources by simple linear parameterizations of brightness proxies (Hoegy et al 1993, Woods & Rottman 1996).

Although solar activity itself exhibits multidecadal and centennial fluctuations, whether sources of solar radiation variability exist over these time scales is unknown. A lack of sunspots in the seventeenth century Maunder Minimum (Figure 2*e*) that was coincident with high cosmogenic isotope concentrations (Figure 2*f*), decreased solar rotation, and increased solar diameter points to

anomalously low solar activity relative to contemporary levels (Eddy 1976, Eddy et al 1976, Gilliland 1981, Nesme-Ribes et al 1993, Fiala et al 1994). That Sun-like stars without apparent activity cycles, possibly analogous to the Maunder Minimum Sun, are less bright than their cycling counterparts (Baliunas & Jastrow 1990) suggests that the Sun's radiation was also depleted during this period (White et al 1992, Lean et al 1992). Proposed mechanisms include reduction of the Sun's chromospheric network and basal emission from supergranule cells (White et al 1992) and reduced convective flow strengths that bring magnetic fields to the Sun's surface (Hoyt & Schatten 1993, Nesme-Ribes et al 1993). More generally, comparisons of solar and stellar radiation suggest that the Sun is potentially capable of a wider range of variability than that which we are witnessing in the contemporary era (Lockwood et al 1992, Haisch & Schmitt 1996, Ayres 1997), but sources of this prospective variability, though speculated, are undetermined (Newkirk 1983).

3.3 *Amplitudes of Solar Radiation Variability*

Measuring the variability of the Sun's radiation spectrum with sufficient reliability to define Sun-Earth coupling processes is a challenging task for contemporary space-based solar monitoring. With this goal, solar irradiance monitors have flown on various spacecraft since the 1970s (Lean 1991), producing, for example, the total, 200-nm, and X-ray irradiance data in Figure 2.

The variability best quantified observationally is that of the Sun's total (spectrally integrated) radiative output. Overlapping cross-calibrated measurements made by active cavity radiometers since November 1978 compose a total irradiance database with sufficient long-term precision to identify an 11-year total irradiance cycle of about 0.1% amplitude during solar cycles 21 and 22, in phase with solar activity (Willson & Hudson 1991, Willson 1994, Lee III et al 1995). The total irradiance cycle may be as much as 0.15% (Hoyt et al 1992, Fröhlich 1994) and may precede the phase of solar activity (Schatten 1988) if trends evident in some portions of the database arise from real solar variability rather than drifts in radiometer sensitivities.

Irradiance variability amplitudes in most parts of the solar spectrum must be deduced from intermittent measurements made with inadequately calibrated instruments that lack in-flight sensitivity monitoring (Lean 1991, Tobiska 1993); these data exist only at wavelengths less than 400 nm and are shown in Figure 5. Most reliable is the $8 \pm 1\%$ irradiance cycle at 200 nm, for which two flight-calibrated instruments on the Upper Atmosphere Research Satellite (UARS) in cycle 22 (Woods et al 1996) agree with earlier Solar Mesosphere Explorer (SME) observations in cycle 21 (Rottman 1988) and with empirical proxy parameterizations (Cebula et al 1992, Lean et al 1997a). At wavelengths longer than 300 nm, the $\pm 1\%$ long-term precision of UARS solar UV monitoring is

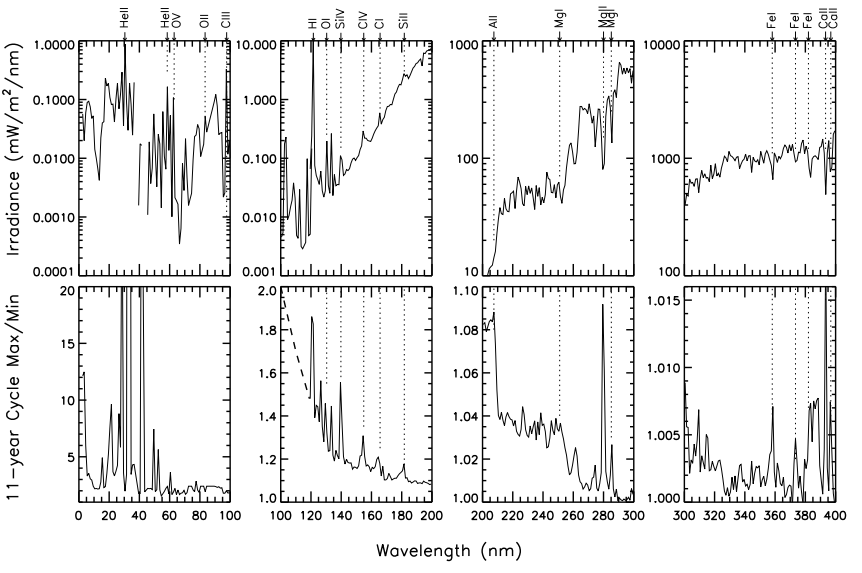

Figure 5 Shown in the upper panel is the Sun's spectral irradiance at wavelengths from 0 to 400 nm and in the lower upper panel its 11-year cycle variability. EUV spectra are obtained from the Hinteregger et al (1981) empirical model, which is based on Atmospheric Explorer-E data. The 100- to 400-nm spectra were measured by SOLSTICE on UARS (Woods et al 1996). At wavelengths longward of 200 nm, the variations are estimates from a proxy variability model that scales the irradiance modulation detected during solar rotation (e.g. Figure 4) to the longer time scale of the 11-year cycle (Lean et al 1997a).

insufficient to detect spectral irradiance variations that are estimated to be less than 1% (Figure 5). In the vicinity of H I 121.5 nm, irradiance changes of 80–100% measured by the UARS instruments exceed proxy model estimates of a 50–60% reduction during the descending phase of solar cycle 22 (Chandra et al 1995) and of the 60% variability measured by SME during cycle 21. The EUV spectral irradiance variability amplitudes, deduced primarily from four years of Atmospheric Explorer-E measurements (Hinteregger et al 1981), exceed factors of two (Figure 5) but are uncertain by 50–100%. In lieu of adequate observational data, empirical variability models estimate irradiances from parameterizations of various solar activity proxies either by fitting the extant database (Hinteregger et al 1981, Tobiska 1993) or by scaling the better-defined rotational modulation to the longer 11-year cycle (Cebula et al 1992, Lean et al 1997a). Poor observational constraints continue to limit the reliability of these models (Lean 1990).

Solar radiation variability amplitudes remain poorly characterized on the very short time scales (minutes to hours) of solar flares, except in certain X-ray bands

measured by GOESS and Yohkoh. Eruptive events in the Sun's atmosphere can cause significant amplitude variations in EUV radiation (White 1977) and possibly in UV emissions as well (Brekke et al 1996), but the time resolution of solar radiation monitoring in general has been insufficient to properly quantify these events.

On multidecadal and centennial time scales, amplitudes of solar irradiance variability are as yet unmeasured. Diagnosed associations between sources of contemporary irradiance variability and appropriate solar activity proxies that extend over longer time spans permit the irradiance reconstructions shown in Figure 6. In addition to the 11-year cycle, a longer-term variability component is postulated to account for a 0.24% irradiance reduction in the Maunder Minimum based on interpretation of Ca II emission from the Sun and Sun-like stars (Lean et al 1995). Other reconstructions yield long-term variability amplitudes that range from 0.1 to 0.6% (Hoyt & Schatten 1993, Nesme-Ribes et al 1993, Jirikowic & Damon 1994, Zhang et al 1994).

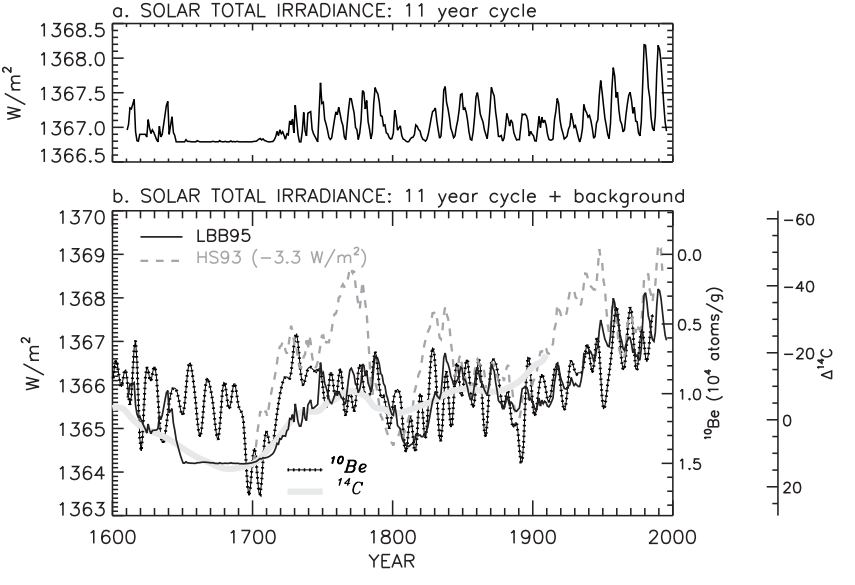

Figure 6 The reconstruction of solar total irradiance shown in (*a*) is of the 11-year cycle alone (Foukal & Lean 1990), whereas the dark solid line in (*b*) combines the 11-year activity cycle and a longer term component based on the average amplitude of each sunspot cycle (Lean et al 1995). This latter irradiance reconstruction is compared with ^{10}Be (*small squares*) and ^{14}C (*thick gray line*) cosmogenic isotope records (Beer et al 1988, Stuiver & Braziunas 1993) and with the Hoyt & Schatten (1993) irradiance reconstruction (*gray dashed line*) in which longer term changes are based on the length of the 11-year solar activity cycle (rather than average amplitude).

4. EARTH'S ABSORPTION OF SOLAR RADIATION

Earth's atmosphere, a blanket of gases extending hundreds of kilometers into space, is relatively transparent to visible and near-IR radiation, allowing some 99% of the Sun's energy—the spectrum longward of 310 nm—to penetrate to below 15 km, into the troposphere where most of the Earth's atmosphere resides, weather and climate occur, and the biosphere exists (Figure 7). The Earth reflects about 30% of this incident solar energy back into space and receives from the remaining 70% a globally averaged energy input of 239 W/m^2 ($1366 \times 0.7/4$ W/m^2). Heated to 255 K by the Sun, the Earth radiates its own energy, which gases in its lower atmosphere—CO_2, H_2O, O_3, N_2O, and CFCs—absorb, trapping additional energy in the troposphere. This greenhouse effect provides further surface warming to 288 K (Peixoto & Oort 1992, Hartmann 1994).

The UV radiation from the Sun also provides significant energy to the terrestrial system, although not in the form of direct surface heating. Energy deposition from radiation at wavelengths less than 310 nm, in the UV, EUV, and X-ray portions of the spectrum, takes place at altitudes shown in Figure 7*a*

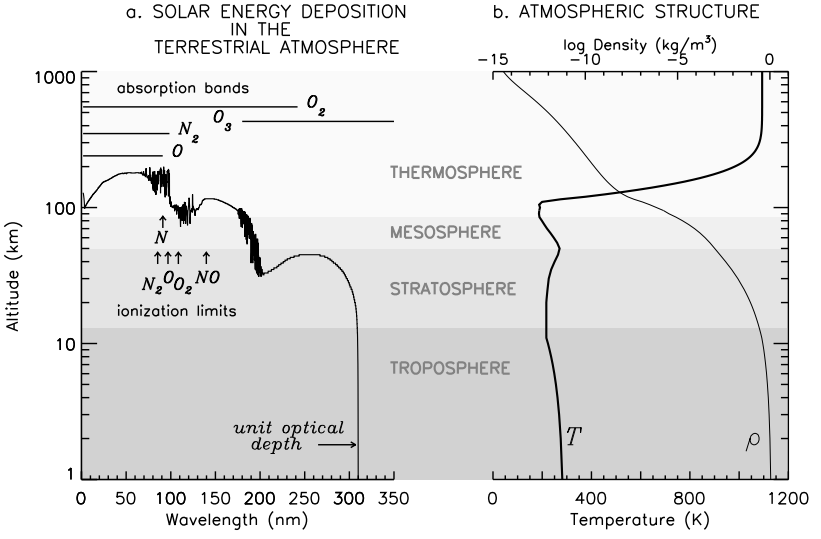

Figure 7 Different regions of the solar spectrum penetrate to different altitudes in the Earth's atmosphere because atmospheric species absorb radiation at different wavelengths. Shown in (*a*) is the altitude at which the Earth's atmosphere attenuates incident radiation from an overhead Sun by a factor of 1/*e* (Meier 1991). Deposited solar energy determines the atmosphere's temperature profile (T) in (*b*), on which atmospheric regions are based.

for the Sun directly overhead, which are determined by the concentrations and absorption cross sections of the primary atmospheric gases (O_2, N_2, O) and O_3 (a minor species) (Meier 1991). Although a mere 1% of the Sun's total radiative output, this radiation controls the overall thermal profile of the atmosphere above about 15 km and much of the chemical, dynamical, and radiative processes occurring there (Banks & Kockarts 1973, Brasseur & Solomon 1984). Ozone absorption of 200- to 300-nm radiation provides sufficient energy to heat the stratosphere from 216 K at altitudes near 15 km to 270 K at 50 km. Molecular oxygen absorption of radiation at wavelengths shorter than 242 nm is a prime energy source for the mesosphere and lower thermosphere (altitudes 75–200 km) and creates oxygen atoms that initiate ozone formation. All three of the upper atmosphere's primary species absorb radiation at wavelengths shorter than 100 nm, providing energy that can heat the thermosphere to more than 1000 K at altitudes above 200 km (Figure 7*b*).

Solar photons at wavelengths less than 102.7 nm have sufficient energy to remove electrons from O_2, N_2, and O (Figure 7*a*). Longer wavelength radiation (primarily H I 121 nm) ionizes NO, and chemical reactions among ions, electrons, and neutrals of major and minor species create additional forms of ionization. As a result, a weakly ionized plasma called the ionosphere is embedded in the neutral upper atmosphere from about 50 to 1000 km (Rishbeth & Garriot 1969).

Both neutral and ionized constituents can transport solar energy from one part of the atmosphere to another, coupling different atmospheric regions with each other and with the Earth's surface. Geographical and altitudinal differences in solar heating drive atmospheric motions that transport heat and chemical species in the lower atmosphere from the tropics to the poles, in Hadley circulation cells. Flows at higher altitudes rise during the summer hemisphere and sink in the winter hemisphere. Turbulent eddy motions and vertical processes such as gravity and planetary waves intermingle with and perturb these meridional motions.

5. SOLAR RADIATIVE FORCING OF GLOBAL CHANGE

Changes in the Earth's global environment—whether caused by the Sun's variable radiation or by other natural or human-made processes—can have ecological, social, and economic consequences (Committee on Earth Sciences 1989, Committee on Environment and Natural Resources 1996). Of paramount concern in the present era are changes arising from anthropogenic influences. Warming of a few degrees Celsius is forecast for Earth's surface temperature in the twenty-first century from increasing concentrations of CO_2 and other greenhouse gases in the atmosphere. Depletion of atmospheric ozone

by CFCs injected into the stratosphere during the past few decades threatens increased surface fluxes of biologically damaging UV radiation [National Research Council 1989, Intergovernmental Panel on Climate Change (IPCC) 1992, 1995].

5.1 *Climate*

Earth's surface temperature, shown in Figure 8*a*, increased 0.7°C over the past 350 years, and 0.5°C since the beginning of the twentieth century. Present levels of annual CO_2 concentrations, shown in Figure 8*b*, are 350 ppm, 27% higher than the 275 ppm preindustrial level (Boden et al 1994). Concentrations of other polyatomic gases—CH_4, N_2O, and CFCs—have also increased, contributing to a 2.4 W/m^2 radiative climate forcing since 1850 (Hansen et al 1993) by trapping IR energy radiated by the Earth to space. This greenhouse gas forcing is identified as the most likely cause of climate change in the past century (IPCC 1995).

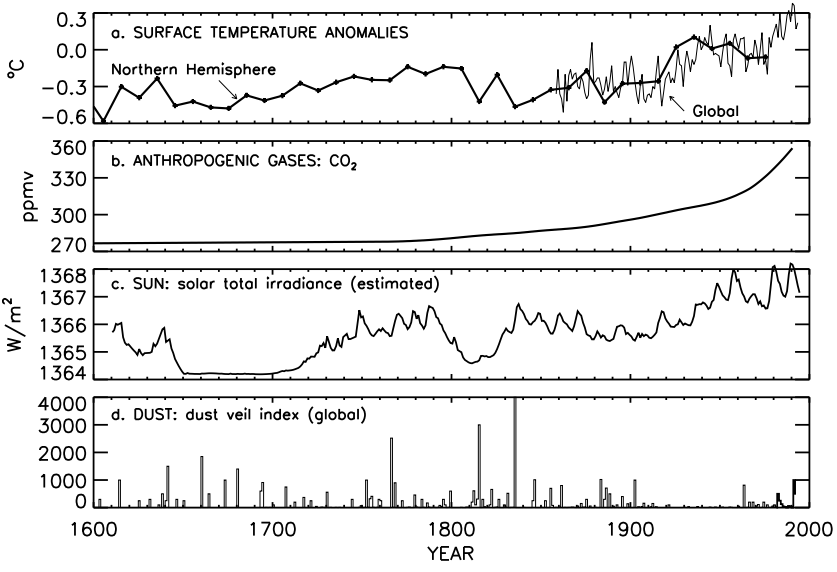

Figure 8 Compared in (*a*) are the Bradley & Jones (1993) reconstructed record of decadal NH surface temperature since 1600 (*solid line with plus signs*) and the IPCC (1992) global instrumental record since 1850 (*thin line*). Both natural and anthropogenic influences may have contributed to the observed surface warming since 1850. Shown are (*b*) annual averages of the concentration of CO_2 (Boden et al 1994), (*c*) estimated solar total irradiance (Lean et al 1995), and (*d*) volcanic aerosol loading according to the global dust veil index (Lamb 1977, Robuck & Free 1995).

Climate adjusts to radiative forcing ΔF by seeking a new thermal equilibrium. Providing the forcing persists long enough for complete adjustment, the accompanying surface temperature change is $\Delta T = \kappa \Delta F$, where κ is the climate system sensitivity. This sensitivity is the net of the various amplification or attenuation processes by which the climate system responds to changes in the energy it receives, depending on the spatial distribution, altitude, and time history of the specific forcing. With κ in the range 0.3–1°C per W/m^2 (Wigley & Raper 1990, IPCC 1995), the greenhouse gas forcing of 2.4 W/m^2 since 1850 should have increased surface temperature in the range of 0.7–2.4°C.

The discrepancy between the observed 0.5°C warming since 1850 and the estimated 0.7–2.4°C greenhouse gas warming cautions that climate change forcings and responses in the industrial era are not yet fully understood. Unlike greenhouse gas forcing, Earth's surface temperature did not increase steadily (Figure 8*a*)—statistical analyses of surface temperatures since 1850 reveal significant decadal and interdecadal variability on global and regional spatial scales (Allen & Smith 1994, Mann & Park 1994, Lau & Weng 1995). Moreover, preindustrial surface temperatures apparently varied independently of greenhouse gas concentrations, which commenced their increase in the nineteenth century.

Other anthropogenic and natural factors likely influenced Earth's climate in the recent past. Figure 9 compares amplitudes of their radiative forcings since 1850, which are known only with very low confidence. Enhanced solar radiative output (Figure 8*c*) may have contributed to surface warming as solar activity increased from the anomalously low activity of the seventeenth century Maunder Minimum. Over the past century, increased industrial aerosol concentrations in the troposphere have potentially cooled Earth's surface by scattering and deflecting incoming solar radiation and by affecting cloud formation (Penner et al 1994, Schwartz & Andreae 1996). Volcanic aerosols in the stratosphere likewise reduce incoming solar radiative energy inputs to the Earth (Robuck & Free 1995). That the atmosphere has been relatively free of volcanic aerosols for most of the twentieth century (Figure 8*d*) implies warmer conditions than in the previous century. Some surface cooling is expected in the past few decades from the depletion of stratospheric ozone by CFCs because ozone is a greenhouse gas (Schwarzkopf & Ramaswamy 1993). Modified patterns of vegetation coverage through human activity have altered surface reflectivity (Hannah et al 1994)—albedo—and the Earth's ability to absorb incoming solar radiation.

In the preindustrial decades from 1610 to 1800, surface temperature anomalies apparently tracked solar activity, increasing 0.26°C as irradiance increased 2 W/m^2 (a 0.35 W/m^2 climate forcing), based on the reconstructed solar irradiance and temperatures shown in Figure 10. Extending this relationship to

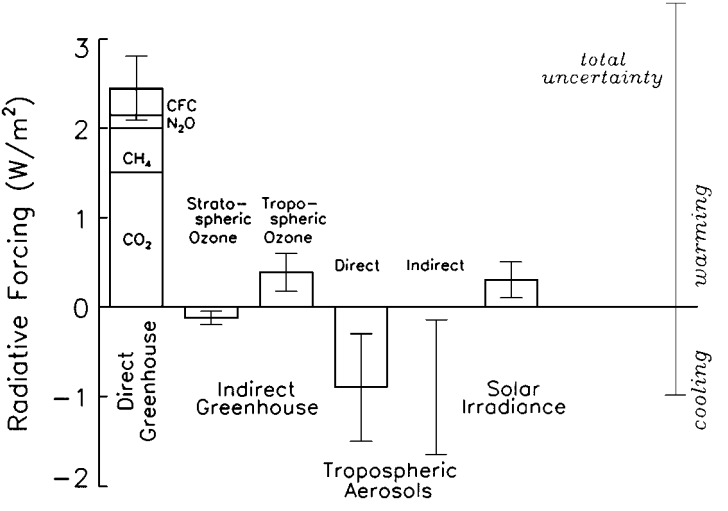

Figure 9 Amplitudes of natural and anthropogenic climate forcings from 1850 to 1990 are shown from IPCC (1995). Each individual forcing is expected to impact the climate system in different ways depending on its latitude, altitude, and history. However, climate change assessments lack the complexity to account for the myriad pathways of the climate system response, and global scale studies often assume a common climate sensitivity to the different forcings.

the present yields a solar induced surface temperature increase of about 0.25°C since 1850, or about half the observed warming. Other empirical studies similarly infer that one third to one half of centennial scale climate change in the recent Holocene may be solar related (Reid 1991, Schlesinger & Ramankutty 1992, Crowly & Kim 1996). Adding further support, a simulation with the Goddard Institute for Space Studies (GISS) general circulation climate model estimates a northern-hemisphere equilibrium surface temperature change of 0.49°C for a 0.25% irradiance reduction (Rind & Overpeck 1993), which is in surprisingly good agreement with the 0.45°C increase since the Maunder Minimum determined empirically from the data in Figure 10. But whether solar total irradiance actually did increase 0.25% over the past 350 years is uncertain, and attributing as much as half of the surface warming since 1850 to solar forcing requires substantial offsetting of greenhouse warming by other mechanisms—aerosol cooling and albedo changes, for example. For these reasons, the reality of solar variability influences on centennial climate change deduced from circumstantial evidence such as the empirical relationship in Figure 10 is controversial.

Solar variability may influence climate on decadal as well as centennial time scales. Cycles of 11 and 22 years exist in a wide variety of contemporary

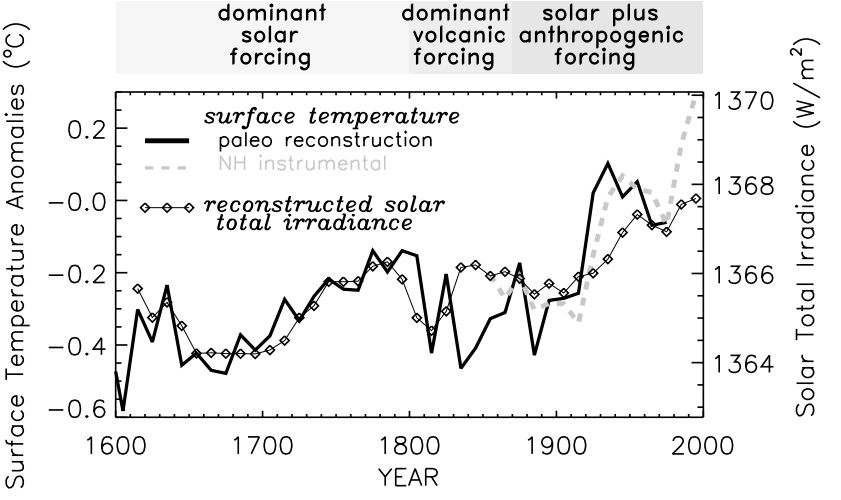

Figure 10 Compared are decadally averaged values of solar total irradiance reconstructed by Lean et al (1995) and NH summer temperature anomalies from 1610 to the present. The dark solid line is the Bradley & Jones (1993) NH summer surface temperature reconstruction from paleoclimate data (primarily tree rings), scaled to match the NH instrumental data (IPCC 1992) (*gray dashed line*) during the overlap period. (Updated from Lean et al 1995.)

climate records, including temperatures of land and ocean surfaces and of the troposphere, US drought, rainfall, forest fires, and cyclones. These cycles also occur in longer-term climate proxy records, including $\Delta^{18}O$ concentrations in ice cores and tropical corals (see Lean & Rind 1997 for references). Since the 1950s, a decadal component in global sea surface temperature, shown in Figure 11, has varied in phase with the 11-year solar activity cycle (White et al 1997), increasing roughly 0.1°C (peak to peak) as solar irradiance increased 1.3 W/m^2 during the two most recent solar cycles. Wavelet transform analysis of the northern-hemisphere temperature record (land plus ocean) likewise detects an 11-year cycle of amplitude ∼0.1°C, which is in phase with solar activity in recent cycles (Lau & Weng 1995).

But like other climate cycles, including the 3- to 7-year El Niño Southern Oscillation band, the 11- and 22-year cycles are capricious (Burroughs 1992). They are neither present in all climate proxy records nor are they always present in any one record or always in phase with the solar activity cycle. Instead of solar variability, an internal oscillation of the ocean-atmosphere system is frequently proposed as the origin of observed decadal climate change (Metha & Delworth 1995). Climate simulations with general circulation models replicate such an oscillation in the absence of any external forcing (James & James 1989),

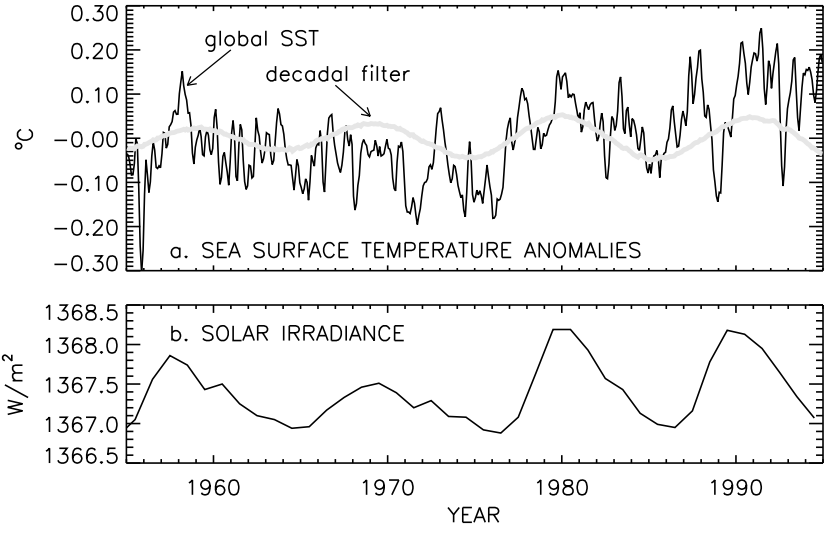

Figure 11 White et al (1997) identified in globally averaged sea surface temperature anomalies compiled from bathythermographs (BT), significant annual and interannual variability including a decadal component shown in (*a*) that tracks solar irradiance reconstructed by Lean et al (1995), shown in (*b*).

although not on the global scale evident in the connections in Figure 11. However, the indication by the GISS general circulation climate model simulation of regional surface temperature inhomogeneities for a 0.25% irradiance reduction may provide an explanation for the non-stationarity of solar-induced decadal cycles—dynamical patterns set up by differential heating of the land and ocean induce regional effects, evolution of which could cause apparent ambiguities in site-specific climate proxy records.

Current climate change theory assumes that the thermal inertia of the oceans prevents the climate system from reaching an equilibrium in response to solar irradiance variations over the 11-year cycle, realizing surface temperature changes of only 0.02–0.03°C (Wigley & Raper 1990, North & Kim 1995), which are factors of three to five smaller than the apparent relationship between decadal solar and global ocean surface temperature fluctuations in Figure 11. There are some indications, however, that the sensitivity of the real climate system to small solar radiative perturbations may be greater and more complex than is presently assumed. Using a recently developed scheme for detecting subtle variability modes in climate parameters, Stevens & North (1996) attributed somewhat larger signals of 0.05°C to 11-year solar forcing in the instrumental surface temperature record since 1850. On much longer time scales, general

circulation climate model simulations of Ice Age occurrences forced by Earth's orbital motions about the Sun (the Milankovitch effect) (Hays et al 1976) cannot account properly for the unexpectedly prominent 100,000-year periodicity in the paleoclimate record, which is associated with the eccentricity of the Earth's orbit (Rind et al 1989). This changing Sun-Earth distance modulates the solar radiation incident on the Earth, as does solar activity.

5.2 *Ozone*

Ozone is Earth's biological UV shield (de Gruijl 1995), as well as a greenhouse gas (National Research Council 1989). Although present in the atmosphere only in trace amounts—about 40 parts per billion volume near the Earth's surface—ozone molecules exert a strong control on, and are in turn affected by, the physical state of the middle atmosphere (Brasseur & Solomon 1984).

Fundamental to the existence of ozone is the interaction of solar UV radiation with atmospheric oxygen compounds. Solar UV radiation at wavelengths less than 242 nm creates oxygen atoms by photodissociating oxygen molecules. Atomic and molecular oxygen combine to produce a layer of triatomic oxygen—ozone—with peak concentrations of 10 ppm at altitudes near 25 km. By photodissociating other atmospheric constituents, solar radiation also creates varieties of hydrogen, nitrogen, oxygen, and chlorine radicals that destroy ozone by catalytic chemical cycles. In particular, solar UV radiation near 200 nm liberates Cl atoms from anthropogenic CFCs that drift up to the middle atmosphere from the Earth's surface (McElroy & Salawitch 1989). And solar radiation itself destroys ozone, which dissociates upon absorption of UV radiation at wavelengths from 200 to 300 nm. This absorption prevents UV photons from reaching the biosphere and supplies the middle atmosphere with energy to drive large-scale dynamical motions that transport atmospheric species to different latitudes and altitudes.

Globally averaged total column ozone concentrations above the Earth's surface, shown in Figure 12, exhibit a long-term downward trend during the past 15 years that is anticipated to enhance fluxes of UVB radiation (290–320 nm) at the Earth's surface (Madronich & deGruijl 1993, Herman et al 1996). This trend is attributed to ozone destruction by CFCs (World Meteorological Organization 1991) and is estimated to be occurring at a rate of $0.27 \pm 0.14\%$ per year (Stolarski et al 1991, Hood & McCormack 1992). Also, industrially produced CO_2 may be cooling the stratosphere (Rind et al 1990, Ramaswamy et al 1996) and impacting ozone through the strong temperature dependence of ozone's reactions with other atmospheric species.

Superimposed on the overall downward ozone trend in Figure 12 are significant ozone fluctuations related to seasonal cycles, the quasibiennial oscillation (known as the QBO) of wind direction in the tropical lower stratosphere,

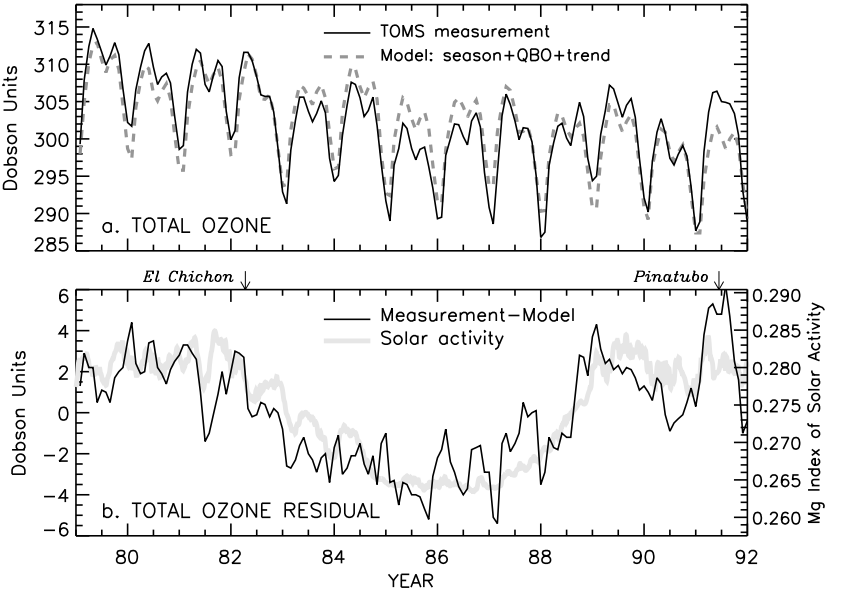

Figure 12 Shown are the results of an analysis of the variability modes evident in global column ozone since 1978, by Hood & McCormack (1992). The Total Ozone Mapping Spectrometer ozone measurements in (*a*) (*solid line*) are compared with a fitted statistical model of seasonal, linear trend, and quasibiennial oscillation terms (*gray dashed line*). The residual of the measured minus model ozone is shown in (*b*) to track the Mg index of solar activity (provided by L Puga, NOAA).

volcanic eruptions, and the 11-year solar activity cycle (Hood & McCormack 1992, Reinsel et al 1994, Randel & Cobb 1994, Solomon et al 1996). These naturally occurring influences combine to almost obscure ozone's long-term depletion since 1979, and they add considerable uncertainty to the deduction of its true magnitude. For example, the increase in solar activity from minimum levels in 1986 to high levels near the cycle 22 maximum in 1990 produced UV radiation enhancements that increased total ozone in the range 1.5 to 1.8% (Wuebbles et al 1991, Hood & McCormack 1992), more than countering the 1.35% anthropogenic depletion over the same five year period.

The impacts of variable solar radiation and other natural and anthropogenic influences on ozone depend on geographical location and altitude. Long-term CFC-induced ozone depletion is pronounced at higher latitudes and at altitudes below the peak ozone concentrations—in the lower stratosphere (Randel & Cobb 1994, Reinsel et al 1994), whereas ozone responds to varying solar radiation mainly in regions where it is photochemically controlled—over the subtropics in the upper stratosphere. Ozone also responds to the apparent

overall response of the middle atmosphere to solar activity through temperature-dependent chemistry and by dynamical transport. Oscillations with periods of 10 to 12 years in phase with solar activity are evident in middle atmosphere temperatures, pressures, and winds. These oscillations vary in strength with geographical locations and altitude and are enhanced at some locations by the phase of the quasibiennial oscillation (Labitzke & van Loon 1992, 1993, Hood et al 1993). However, the sparseness and brevity of comprehensive, global middle atmosphere data prompts questions about the robustness of these relationships (Salby & Shea 1991) and the reality of solar-induced decadal scale variability in the middle atmosphere is still somewhat controversial, although less so than in the lower atmosphere.

Middle atmosphere theory can account for only some of the empirical connections evident among solar variability, ozone and the middle atmosphere. Coupled two-dimensional chemical-dynamical models do predict that enhanced UV radiation near maxima of the 11-year solar cycle increases ozone in the upper stratosphere, but by about a factor of two less than the 5–7% observed enhancement (Chandra & McPeters 1994). Agreement between models and measurements is better for the shorter 27-day solar rotational modulation (Fleming et al 1995). But these models fail to account for emerging empirical evidence of solar-induced fluctuations in the lower stratosphere (Reinsel et al 1994, Hood 1997), which are thought to arise from dynamical amplification of the initial solar radiative forcing of ozone (Hood et al 1993). Nor do they simulate adequately the coupling of solar-induced variability in the lower thermosphere with the middle atmosphere. When transported to the stratosphere in the polar night, enhanced levels of NO produced in the lower thermosphere by solar EUV radiation and X rays during high solar activity are calculated to destroy sufficient ozone such that total column concentrations vary out of phase with solar activity (Brasseur 1993), in contrast to observations (Figure 12).

Whether caused by anthropogenic or natural influences, changes in middle atmosphere ozone and heating have the potential to impact climate in the troposphere through radiative and dynamic coupling processes. Key to these putative impacts are changes in ozone's vertical concentration profile. Depending on altitude, such changes can affect absorption of both solar UV and terrestrial IR energy, producing either a net cooling or warming of the Earth's surface (Lacis et al 1990). In addition, model simulations of solar-induced wind and temperature patterns in the stratosphere produce thermal gradients between the troposphere and stratosphere that alter the strength of tropospheric Hadley cell circulation and the generation and propagation of planetary waves around the globe, which affects weather and climate (Haigh 1994, 1996, Rind & Balachandran 1995).

6. SPACE WEATHER IMPACTS OF SOLAR RADIATION

Solar-extreme and far-UV radiation (at wavelengths less than 170 nm) is the upper atmosphere's primary energy input and creates, as well, its embedded ionosphere (Banks & Kockarts 1973). Unlike the subpercent fluctuations typical of the visible and IR radiative energy inputs to the lower atmosphere, solar EUV radiation exhibits substantial variability, of factors of two or more (Figure 5), that alters significantly the thermodynamic, chemical, and radiative state—the "weather"—of the thermosphere (Roble & Emery 1983) and ionosphere (Ratcliffe 1972, Jursa 1985). During the Sun's 11-year activity cycle, upper atmosphere temperatures (shown in Figure 13) fluctuate by factors of two, and neutral and electron densities by factors of ten. These solar-induced changes exceed by two orders of magnitude the suspected decadal

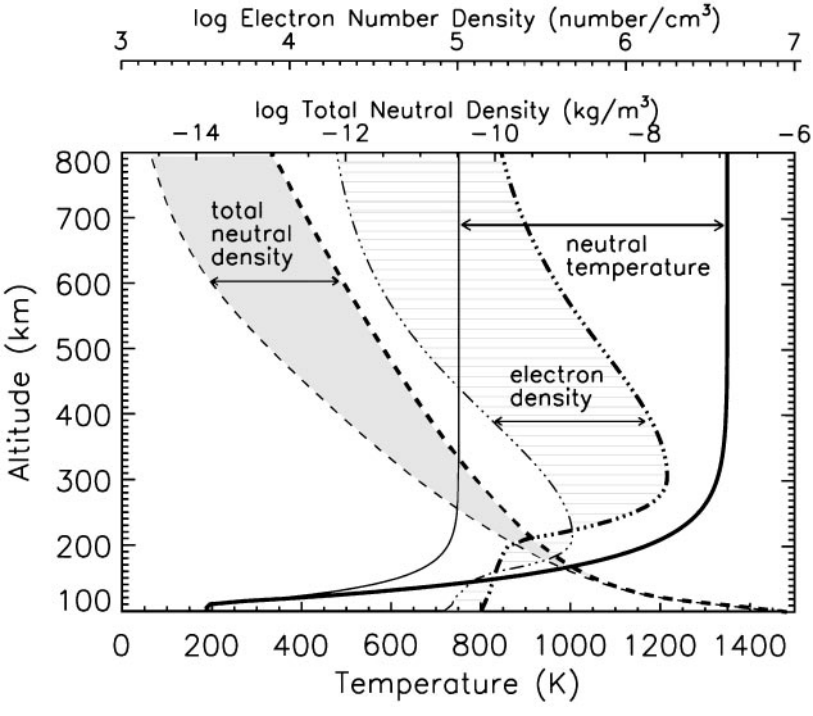

Figure 13 Increases in extreme and far UV radiation from low ($F_{10.7} = 70$) to high ($F_{10.7} = 230$) solar activity heats the entire upper atmosphere and increases total neutral and electron densities by more than an order of magnitude. The Mass Spectrometer and Incoherent Scatter (MSIS) and International Reference Ionosphere (IRI) models were used to calculate these profiles.

anthropogenic impact of greenhouse gas cooling on either upper atmosphere temperatures or densities (Rishbeth & Roble 1992, Bremer 1992). As a fundamental driver of space weather at altitudes between 50 and 1000 km, the Sun's variable EUV radiation is of socioeconomic relevance (National Space Weather Program 1995)—its variability can affect the operation and performance of complex space-borne systems and networks utilized with increasing reliance for national and societal needs of communication, navigation, surveillance, and commerce (Goodman & Aarons 1990, Gorney 1990, Lanzerotti 1994).

6.1 *Spacecraft*

Including spacecraft and debris, more than 8000 catalogued objects now orbit the Earth in both circular and elliptical orbits at altitudes ranging from a few hundred to many thousands of kilometers (Committee on Transportation Research and Development 1995). Depending on its velocity and ballistic coefficient, an Earth-orbiting object experiences deceleration due to friction with the upper atmosphere that limits its lifetime (King-Hele 1987). Unboosted spacecraft in circular orbits at altitudes less than 500 km eventually reenter the Earth's atmosphere, usually burning up and generating additional debris, as was the case for the Solar Maximum Mission (Covault 1989), but sometimes impacting the Earth's surface, as did SkyLab in 1979.

"Drag" on an object at a given altitude depends on the density of the upper atmosphere, which, as seen in Figure 13, is not constant. Responding to elevated heating by enhanced EUV and UV radiation during times of high solar activity, the atmosphere expands outward from the Earth, bringing higher densities to a given altitude. Density fluctuations also occur with somewhat smaller amplitudes on time scales of days and months (White et al 1994), primarily in response to the Sun's 27-day rotational modulation of EUV radiation. As an example, atmospheric drag on the Solar Maximum Mission spacecraft in the vicinity of 400 km during a period of moderate solar activity, shown in Figure 14 just prior to reentry, caused orbital decay rates as high as 0.5 km/day near radiation peaks of the 27-day cycle.

Efficient planning, management, and operation of space-based resources require the ability to specify and forecast the orbits of both spacecraft and debris (for collision avoidance) (Space Environment Services Center 1982). On multiyear time scales, this capability benefits planning for mission resources such as operations, battery storage, and fuel loadings (NASA 1994), and it is needed for coordinating the construction and maintenance of the International Space Station (ISS). At a planned orbital altitude of 400 km, ISS is scheduled to commence operation at near record high levels of activity predicted for solar cycle 23 maximum, and it will require periodic reboosting throughout its multidecadal

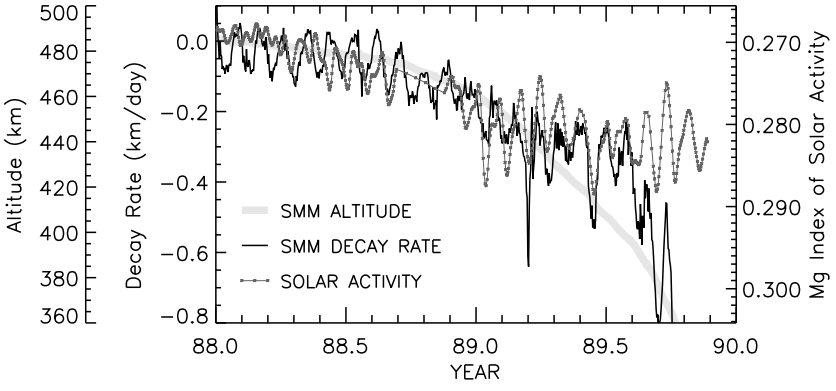

Figure 14 Superimposed on the overall orbital decay of the Solar Maximum Mission (SMM) spacecraft at altitudes from 490 to 360 km (*thick gray line*) are notable fluctuations in decay rate (*thin dark line*) associated with modulation of the Sun's EUV radiation by solar rotation, indicated by the Mg index proxy (*gray stars*). (D Messina provided the SMM altitude data, and L Puga the Mg indices.)

operational lifetime. During the previous solar cycle 22, inadequacies of the current state of the art for predicting solar activity and the response of the upper atmosphere to attendant EUV radiation fluctuations caused alarm that launch of the Hubble Space Telescope into low Earth orbit at that time would severely curtail its lifetime (Withbroe 1990). Orbital anomalies and premature vehicle reentry arising from uncertainties in upper atmosphere densities are also of economic concern for commercial ventures, which propose to utilize arrays of small, low Earth orbit spacecraft for global communications networks (e.g. IRIDIUM).

When differences between predicted and observed positions of space objects from one orbit to the next exceed specified tolerances, near real-time decisions must be made by the US Air Force and Naval Space Commands (which have responsibility for operational tracking of objects in Earth orbit) to attribute the anomaly to either unexpected atmospheric drag or object misidentification. Minimizing uncertainties in orbital tracking due to atmospheric drag can help reduce the occurrence of such anomalies and also improve the accuracies of alerts and warnings of potential collisions between spacecraft, such as that witnessed recently between two orbiting objects (David 1996). Collisions with orbital debris is a serious issue for the ISS because maneuvering to avoid infrastructure damage will perturb the microgravity and aspect environments for ISS experiments.

Incorporating into operational orbital tracking tools state-of-the-art upper atmosphere density models promises to reduce uncertainties in the locations of

spacecraft and debris. In lieu of routine solar EUV irradiance measurements for input, present semi-empirical upper atmosphere models such as those of Jacchia (1977) and MSIS (Mass Spectrometer and Incoherent Scatter) (Hedin 1991) utilize the 10.7-cm radio flux as a proxy. Since four of the five strongest solar emission lines that heat the thermosphere (Roble 1987) emerge from the Sun's chromosphere, adopting a chromospheric proxy for solar EUV radiation variability rather than the primarily coronal 10.7-cm radio flux may help improve these models. One candidate is the Mg index proxy (L Puga, private communication) used in Figure 14.

6.2 *Communication*

Electrons in the Earth's ionosphere form conducting layers that inhibit the dissipation to space of radio waves transmitted upward from the surface at certain frequencies, reflecting them instead. This process enables communications from one site to another around the globe, first demonstrated by Marconi in 1901, as well as from spacecraft to the ground and between spacecraft (Goodman 1992).

Different ionospheric layers play different roles in either facilitating or impeding radio communications over a range of frequencies (Jursa 1985). Electron concentrations peak at a few hundred kilometers above the Earth's surface (Figure 13). This uppermost ionospheric layer, called the F region, reflects high frequencies (3–30 MHz) that have a range of 100 to 10 m and are utilized for broadcasting and over-the-horizon radar surveillance. Electrons at lower altitudes—95 to 140 km, in the E region—reflect medium frequencies (300–3000 kHz) with wavelengths 1 to 0.1 km. Although absorbed by the underlying D region during the daytime, medium frequency waves can propagate considerable distances during the night. Electrons at heights less than 90 km ($<$75 km during the daytime) reflect low and very low frequencies (3–300 kHz), which facilitate communication over distances ranging from several hundred to many thousands of kilometers that are used primarily by the military for navigation and surveillance. Electron and ion densities that are present over a very large range of altitudes—above 50 km—affect extremely low frequencies, which can propagate on a global scale.

Management of the frequency spectrum to ensure uninterrupted communication among different sites on the globe requires operational specification of the ability of the ionosphere to reflect or absorb radio waves at different frequencies. This depends on the total number and height distribution of electrons, which depend, in turn, on the field of solar ionizing radiation. Diurnal, seasonal, and solar activity cycles are thus critical factors that determine the state of the ionosphere and electron concentrations at a given altitude and geographical location (Rishbeth & Garriott 1969).

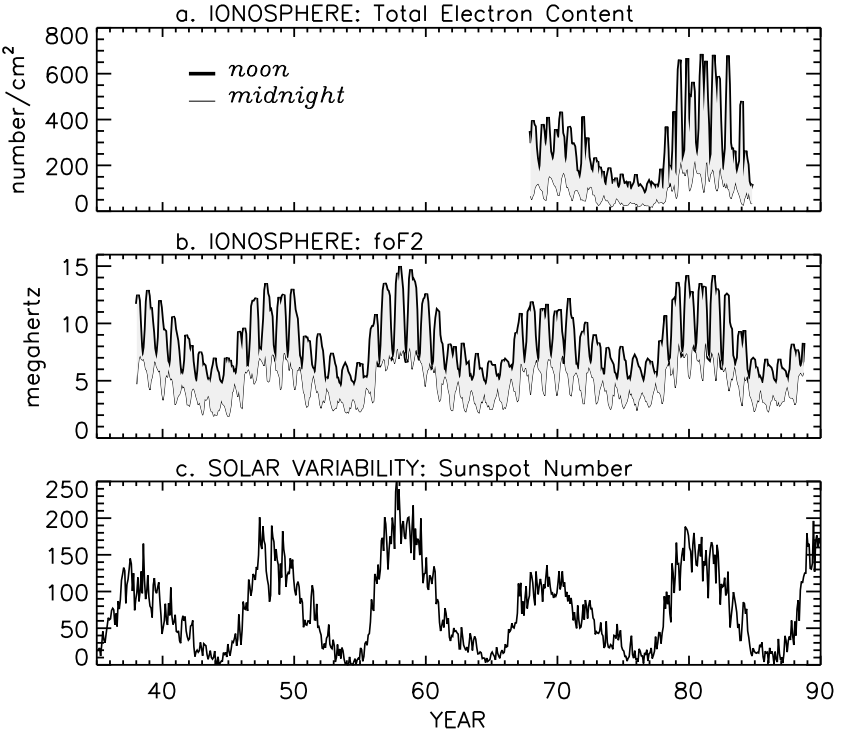

Figure 15 The 11-year cycle in solar EUV radiation produces significant changes in the ionosphere, including in (*a*) the total number of electrons and (*b*) the critical frequency, foF2, above which radio waves are lost because the ionosphere is unable to reflect them to Earth (Davies & Conkright 1990). (Data provided by R Conkright of NOAA's WDC.)

Changing levels of solar activity continuously alter EUV and X-ray ionization rates, and hence electron concentrations, in the atmosphere on time scales from minutes to the 11-year cycle (Balan et al 1994). For example, the limiting or critical frequency, foF2, above which a radio wave is no longer reflected by an ionized atmospheric layer, depends on the square root of the electron density in the layer, and this in turn varies with the intensity of the ionizing radiation. Monthly averaged noontime foF2 values are seen in Figure 15 to vary from 6 to 12 MHz as total electron column increases by factors of more than five from low to high solar activity levels, as indicated by the sunspot number (Davies & Conkright 1990).

Less regular, sudden ionospheric disturbances (SIDs) occur when solar flare enhancements of X-ray and short-wavelength EUV emission cause rapid

increases in D-region electron concentrations, thickening this lowest ionospheric region and lowering the height of maximum electron density on the sunlit side of the Earth. Major operational impacts of SIDs last from minutes to a few hours. These include fadeouts and frequency increases of high frequency waves, which experience increased absorption as they pass through the D region and encounter increased ionization in the E and F regions. Phase anomalies, sudden signal enhancements, and increased background noise occur in communications at very low frequencies in response to the lowering and strengthening of the D region, which affect the accuracies of navigation systems that use these frequencies (LORAN and OMEGA).

Total electron content is also of great importance to precision satellite-based positioning systems such as Global Positioning Systems (GPS), Very Long Baseline Interferometry (VLBI), and Satellite Laser Ranging (SLR) because the ionosphere is a dispersive medium with respect to the radio signals that they employ (Vallance Jones 1993). Since the time delay in the information carried by a wave depends on its frequency, the use of dual frequencies at fairly widely spaced bands reduces errors by eliminating ionospheric refraction. But much navigation and positioning still relies on a single frequency for which specification is needed of the variable total electron content and its rate of change along a path from receiver to transmitter—quantities that are strongly affected by variable solar EUV radiation. Like the upper atmosphere neutral density models, empirical and operational ionospheric models utilize either the 10.7-cm flux or the sunspot number as proxies for the geophysically relevant but observationally unavailable EUV irradiances.

7. SUMMARY

Numerous associations are evident between solar variability and terrestrial parameters that range from the Earth's surface to hundreds of kilometers above it, on time scales from days to centuries. Global solar and terrestrial parameters derived from space-based and ground-based monitoring, primarily in the past few decades, are facilitating renewed efforts, begun over a century ago, to authenticate apparent Sun-Earth connections by deducing their physical mechanisms.

Decadal cycles in phase with the Sun's activity are evident in temperatures at the Earth's surface and throughout the atmosphere, from the troposphere to the thermosphere. Also apparent is an association of surface temperature with overall solar activity during the past few centuries. But whether the Sun's variable radiation is responsible for these connections is in many instances ambiguous. Confidence in this hypothesis increases with height above the Earth's surface, as the variability of the solar radiative energy deposited there increases and the density of the atmosphere decreases. Least certain is the extent to

which tenths percent changes in visible and IR radiation modify global surface temperature and climate, in competition with impacts of other natural and anthropogenic influences. Higher, in the middle atmosphere, there is now cautious confidence that 11-year UV radiation cycles with amplitudes of a few percent do indeed drive changes in temperature, ozone, and winds—associations that were originally debunked in the 1970s as "autosuggestions." In fact, global column ozone concentrations vary during the 11-year cycle by amounts comparable to anthropogenic CFC depletion over the same period. The control of upper atmosphere temperature, density, and ionization by solar EUV radiation is undisputed. But for lack of global upper atmosphere data and coincident EUV irradiance monitoring, the mechanistic details are insufficiently developed for assessment and forecasting needed in spacecraft and communication management, which continues to rely on radio flux or sunspot number proxies.

During the past few decades, minima to maxima amplitudes of solar activity cycles have been near the largest in the 400-year record, and the overall activity level of the Sun is at a historically high level. Historically high levels of radiation are assumed, too, based on the dependence of the Sun's radiative output on the level of solar activity. Although prediction of the course of future solar activity with any certainty is not yet possible, the Sun's radiation will undoubtedly continue to vary, potentially impacting the Earth's surface temperature, ozone concentrations, and upper atmosphere composition in the future. With greenhouse gas concentrations forecast to be double preindustrial levels sometime in the twenty-first century, rigorous attribution of all climate forcings and effects will be needed on regional and global scales to secure reliable early warning of the anticipated climatic impacts. Equally challenging will be evaluation of CFC restrictions implemented in the late 1980s to arrest further ozone depletion. Future monitoring of the expected recovery of ozone to pre-anthropogenic concentration levels must account for natural variability induced by the Sun's variable UV radiation. And in the International Space Station era, the ever-growing amount of orbital space debris will increase the urgency to specify solar radiation impacts on upper atmosphere neutral and ion densities to secure efficient utilization and protection of space-based national and commercial assets.

Critical for these tasks is knowledge of solar radiation variability during the 11-year cycle and over the longer term. To secure this knowledge, continuous, reliable space-based monitoring of the Sun's total and spectral irradiance for the indefinite future is necessary, with instruments that have notably improved accuracy and long-term precision relative to the present state of the art. Complementary coordinated studies of the Sun's global radiation variability mechanisms—both magnetic and nonmagnetic, over a wide range of times scales—are needed to identify the sources of variability and to secure

physically justifiable relationships with more widely available solar activity proxies. These studies must develop an understanding of connections between global solar radiative output and continually erupting, evolving, and decaying magnetic fields in the Sun's atmosphere. A lack of such global connections will obfuscate efforts to better quantify the terrestrial relevance of the Sun's variable radiation.

Equally critical are investigations and model simulations of the Earth's response at its surface and throughout its atmosphere to changes in incoming radiation from the Sun over many time scales. Present inability to adequately quantify all climate and ozone forcings adds ambiguities to assessments of the causes of recent global change and cautions against neglect of natural and anthropogenic contributions other than by increasing concentrations of greenhouse gases and CFCs. Improved knowledge of how the terrestrial system itself has varied in the recent past and how forcings in one regime couple to another will help in this effort.

Both the Sun and the Earth exhibit complex, multifaceted, nonlinear, nonstationary variabilities. Neither entities are yet understood sufficiently well to define the causes of their individual variabilities or the impacts of the one on the other. Difficulties inherent in this endeavor should not be underestimated: Caution is required before dismissing empirical associations for lack of understanding within the paradigm of incomplete models, and focused interdisciplinary studies should lead to future progress. Over a decade ago, Evans (1982) characterized the topic of the Sun's relevance for Earth at that time as "intriguing, tantalizing, and far from settled." Although still not settled, the advent of global solar and terrestrial data sets and advances in interpretive and theoretical techniques are enticing new and fruitful explorations of the intrigue and speculation with the added imperative of the recognized societal relevance of Sun-Earth links.

ACKNOWLEDGMENTS

Discussions with many solar and terrestrial physicists over the past decade, and data kindly provided by many more, have benefited this review considerably. Particularly valued are ongoing collaborations with Peter Foukal, David Rind, Dick White, Andy Skumanich, Bill Livingston, Gary Rottman, Tom Woods, Claus Fröhlich, John Cook, Warren White, Ray Bradley, and Juerg Beer. The National Oceanic and Atmospheric Administration World Data Center and its staff, especially Helen Coffey, Dan Wilkinson, and Ray Conkright, have provided continued support for solar terrestrial data requests: Ray Conkright provided the ionospheric data in Figure 15. Loren Acton and Keith Strong have helped in discussing Yohkoh SXT data. Bill Marquette and Anders Johannesson

supplied Ca K images, Dick Willson the total irradiance data, Minze Stuiver the ^{14}C data in Figure 2, Warren White the SST data in Figure 11, Larry Puga the Mg index data in Figures 12 and Figures 14, and Lon Hood the ozone data in Figure 12. Harry Warren helped with accessing Ca K and GOES data. Lee Kyle, John Hickey, and Doug Hoyt answered many questions and provided the Nimbus 7 solar filter data. Owen Kelley ran the IRI model to generate the ionospheric data used in Figure 13. The NRL's Space Science Division provides a stimulating environment for investigations of this topic in ongoing interactions among members of its Solar Terrestrial Relationships and Upper Atmospheric Physics Branches—Bob Meier, Mike Picone, John Mariska, and Dave Siskind. In addition to numerous discussions, some members of these branches read parts of the text. NASA's Space Physics Supporting Research and Technology and Mission to Planet Earth UARS Guest Investigator programs jointly funded this review.

Literature Cited

Acton LW. 1996. In *Proc. 9th Coolstar Workshop*, 3–6 October 1995. Florence, Italy
Allen MR, Smith LA. 1994. *Geophys. Res. Lett.* 21:883–86
Angell JK, Korshover J. 1973. *Mon. Weather Rev.* 101:426–43
Ayres TR. 1997. *J. Geophys. Res.* 102:1641–51
Balan N, Bailey GJ, Jenkins B, Rao PB, Moffett RJ. 1994. *J. Geophys. Res.* 99:2243–53
Baliunas S, Jastrow R. 1990. *Nature* 348:520–23
Banks PM, Kockarts G. 1973. *Aeronomy.* New York & London: Academic. Part A, 430 pp. Part B, 355 pp.
Beer J, Siegenthaler U, Bonani G, Finkel RC, Oeschger H, et al. 1988. *Nature* 331:675–79
Boden TA, Kaiser DP, Sepanski RJ, Stoss FW, eds. 1994. *Trends'93: A Compendium of Data on Global Climate Change.* Carbon Dioxide Information Analysis Center. Publ. No. ORNL/CDIAC–65, Oak Ridge Natl. Lab., Oak Ridge, Tenn.
Bradley RS, Jones PD. 1993. *Holocene* 3(4): 367–76
Brasseur G. 1993. *J. Geophys. Res.* 98:23079–90
Brasseur G, Solomon S. 1984. *Aeronomy of the Middle Atmosphere.* Dordrecht: Reidel. 441 pp.
Brekke P, Rottman GJ, Fontenla J, Judge PG. 1996. *Astrophys. J.* 468:418–32
Bremer J. 1992. *J. Atmos. Terrestr. Phys.* 54: 1505–11
Burroughs WJ. 1992. *Weather Cycles Real or Imaginary?* Cambridge: Cambridge Univ. Press. 207 pp.
Cebula RP, DeLand MT, Schlesinger BM. 1992. *J. Geophys. Res.* 97:11613–20
Chandra S, Lean JL, White OR, Prinz DK, Rottman GJ, Brueckner GE. 1995. *Geophys. Res. Lett.* 22:2481–84
Chandra S, McPeters RD. 1994. *J. Geophys. Res.* 99:20665–71
Committee on Earth Sciences. 1989. *Our Changing Planet: The FY 1990 Research Plan.* US Global Change Res. Prog. Washington, DC: Fed. Coord. Council Sci. Eng. Technol.
Committee on Environment and Natural Resources. 1996. *Our Changing Planet: The FY 1996 U.S. Global Change Research Plan.* Washington, DC: Natl. Sci. Technol. Council
Committee on Transportation Research and Development. 1995. *Interagency Report on Orbital Debris.* Washington, DC: Off. Sci. Technol. Policy
Cook JW, Brueckner GE, VanHoosier ME. 1980. *J. Geophys. Res.* 85:2257–68
Covault C. 1989. *Aviation Week Space Technol.* Oct. 16:23–24
Cox AN, Livingston WC, Matthews MS, eds.

1991. *Solar Interior and Atmosphere.* Tucson: Univ. Arizona Press. 1403 pp.
Crowley TJ, Kim K-Y. 1996. *Geophys. Res. Lett.* 23:359–62
David L. 1996. *Space News* Aug. 26–Sept. 1:4, 19
Davies K, Conkright R. 1990. In *The Effect of the Ionosphere on Radiowave Signals and System Performance,* ed. JM Goodman, pp. 1–11. Ionospheric Effects Symp., Govt. Print. Off. 1990 0-278-020
de Gruijl FR. 1995. *Consequences* 1:13–21
Donnelly RF. 1976. *J. Geophys. Res.* 81:4745–53
Dupree AK, Huber MCE, Noyes RW, Parkinson WH, Reeves EM, Withbroe GL. 1973. *Astrophys. J.* 182:321–33
Eddy JA. 1976. *Science* 192:1189–202
Eddy JA, Gilman PA, Trotter DE. 1976. *Solar Phys.* 46:3–14
Ellison MA. 1969. *The Sun and Its Influence.* New York: Elsevier. 240 pp.
Evans JV. 1982. *Science* 216:467–74
Fiala AD, Dunham DW, Sofia S. 1994. *Solar Phys.* 152:97–104
Fleming EL, Chandra S, Jackman CH, Considine DB, Douglass AR. 1995. *J. Atmos. Terr. Phys.* 57:333–65
Foukal P. 1990. *Solar Astrophysics.* New York: Wiley. 475 pp.
Foukal P, Lean J. 1990. *Science* 247:556–58
Friis-Christensen E, Lassen K. 1991. *Science* 254:698–700
Fröhlich C. 1994. In *The Sun as a Variable Star,* IAU Colloquium 143, ed. JM Pap, C Fröhlich, HS Hudson, SK Solanki, pp. 28–36. Cambridge: Cambridge Univ. Press. 355 pp.
Gilliland R. 1981. *Astrophys. J.* 248:1144–55
Goodman JM. 1992. *HF Communications Science and Technology.* New York: Van Nostrand Reinhold. 631 pp.
Goodman JM, Aarons J. 1990. *Proc. IEEE* 78:512–27
Gorney DJ. 1990. *Rev. Geophys.* 28:315–36
Gurman JB, Delaboudinière JP, Artzner G, Garbiel A, Maucherat A, et al. 1996. *Bull. Am. Astron. Soc.* 28:880 (Abstr.)
Haigh JD. 1994. *Nature* 370:544–46
Haigh JD. 1996. *Science* 272:961–84
Haisch B, Schmitt JHMM. 1996. *Publ. Astron. Soc. Pac.* 108:113–29
Hannah L, Lohse D, Hutchinson C, Carr JL, Lankerani A. 1994. *Ambio* 23:246–50
Hansen J, Lacis A, Ruedy R, Sato M, Wilson H. 1993. *Natl. Geogr. Res. Explor.* 9:142–58
Hara H. 1996. *Structures and heating mechanisms of the solar corona.* PhD thesis. Natl. Astronom. Obs., Japan. 164 pp.
Hartmann DL. 1994. *Global Physical Climatology.* San Diego: Academic. 411 pp.
Hartmann DL, Barkstrom BR, Crommelynck D, Foukal P, Hansen JE, et al. 1993. *Earth Obs.* 5:23–27
Harvey KL, Harvey JW, Martin SF. 1975. *Solar Phys.* 40:87–102
Hays JD, Imbrie J, Shakleton NJ. 1976. *Science* 194:1121–32
Hedin A. 1991. *J. Geophys. Res.* 96:1159–72
Herman JR, Bhartia PK, Ziemke J, Ahmad Z, Larko D. 1996. *Geophys. Res. Lett.* 23:2117–20
Hinteregger HE. 1970. *Ann. Géophys.* 26:547–54
Hinteregger HE, Fukui K, Gilson BG. 1981. *Geophys. Res. Lett.* 8:1147–50
Hoegy WR, Pesnell WD, Woods TN, Rottman GJ. 1993. *Geophys. Res. Lett.* 20:1335–38
Hood LL. 1997. *J. Geophys. Res.* 102:1355–70
Hood LL, Jirikowic JL, McCormack JP. 1993. *J. Atmos. Sci.* 50:3941–58
Hood LL, McCormack JP. 1992. *Geophys. Res. Lett.* 19:2309–12
Hoyt DV. 1979. *Rev. Geophys. Space Phys.* 17: 427–58
Hoyt DV, Kyle HL, Hickey JR, Maschhoff RH. 1992. *J. Geophys. Res.* 97:51–63
Hoyt DV, Schatten KH. 1993. *J. Geophys. Res.* 98:18895–906
Hoyt DV, Schatten KH, Nesmes-Ribes E. 1994. *Geophys. Res. Lett.* 21:2067–70
Hudson HS. 1987. *Rev. Geophys.* 25:651–62
Hudson HS. 1988. *Annu. Rev. Astron. Astrophys.* 26:473–507
Intergovernmental Panel on Climate Change (IPCC). 1992. *Climate Change 1992. Suppl. Rep IPCC Sci. Assess.,* ed. JT Houghton, BA Callander, SK Varney. Cambridge, MA: Cambridge Univ. Press
Intergovernmental Panel on Climate Change (IPCC). 1995. *Climate Change 1994, Radiative Forcing of Climate Change and an Evaluation of the IPCC 1992 Emission Scenarios,* ed. JT Houghton, LG Meira Filho, J Bruce, H Lee, BA Callander, E Haites, N Harris, K Maskell. Cambridge, MA: Cambridge Univ. Press
Jacchia LG. 1963. *Rev. Mod. Phys.* 35:973–91
Jacchia LG. 1977. *Thermospheric temperature, density, and composition models.* Smithsonian Astrophysical Observatory Special Report 375, Cambridge, Mass.
James IN, James PM. 1989. *Nature* 342:53–55
Jirikowic JL, Damon PE. 1994. In *The Medieval Warm Period,* ed. MK Hughes, HF Diaz, pp. 309–16. Dordrecht: Kluwer Academic. 342 pp.
Jursa AS, ed. 1985. *Handbook of Geophysics and the Space Environment.* Air Force Geophys. Lab., Air Force Syst. Command.
Kelly PM, Wigley TML. 1992. *Nature* 360: 328–30

King-Hele D. 1987. *Satellite Orbits in an Atmosphere: Theories and Applications.* Glasgow, London: Blackie
Kuhn JR, Libbrecht KG. 1991. *Astrophys. J.* 381:L35–37
Kyle HL, Hoyt DV, Hickey JR, Maschhoff RH, Vallette BJ. 1993. *NASA Ref. Publ. 1316*
Labitzke K, van Loon H. 1992. *Geophys. Res. Lett.* 19:401–3
Labitzke K, van Loon H. 1993. *Ann. Geophys.* 11:1084–94
Lacis AA, Wuebbles DJ, Logan JA. 1990. *J. Geophys. Res.* 95:9971–81
Lamb HH. 1977. *Clim. Monit.* 6:57–67
Lanzerotti LJ. 1994. In *Solar Terrestrial Energy Program*, ed. DN Baker, VO Papitashvili, MJ Teague, pp. 547–55. COSPAR Colloquia Series, 5. Oxford, UK: Pergamon
Lau K-M, Weng H. 1995. *Bull. Am. Meteorol. Soc.* 76:2391–402
Lean J. 1990. *J. Geophys. Res.* 95:11933–44
Lean J. 1991. *Rev. Geophys.* 29:505–35
Lean J, Beer J, Bradley R. 1995. *Geophys. Res. Lett.* 22:3195–98
Lean J, Rind D. 1997. *J. Climate.* In press
Lean J, Skumanich A, White OR. 1992. *Geophys. Res. Lett.* 19:1591–94
Lean JL, Cook J, Marquette W, Johannesson A, Willson RC. 1997b. *Astrophys. J.* In press
Lean JL, Rottman GJ, Kyle HL, Woods TN, Hickey JR, Puga LC. 1997a. *J. Geophys. Res.* In press
Lee III RB, Gibson MA, Wilson RS, Thomas S. 1995. *J. Geophys. Res.* 100:1667–75
Lockwood GW, Skiff BA, Baliunas SL, Radick RR. 1992. *Nature* 360:653–55
Madronich S, de Gruijl FR. 1993. *Nature* 366: 23
Mann ME, Park J. 1994. *J. Geophys. Res.* 99: 25819–33
Mariska JT. 1992. *The Solar Transition Region*, ed. RF Carswell, DNC Lin, JE Pringle, Cambridge Astrophys. Ser. 23. Cambridge, MA: Cambridge Univ. Press
McElroy MB, Salawitch RJ. 1989. *Science* 243:763–70
McHargue LR, Damon PE. 1991. *Rev. Geophys.* 29:141–58
Meadows AJ. 1975. *Nature* 256:95–97
Meier RR. 1991. *Space Sci. Rev.* 58:1–185
Metha VM, Delworth T. 1995. *J. Clim.* 8:172–90
NASA. 1994. *The Natural Space Environment: Effects on Spacecraft.* NASA Ref. Publ. 1350, Marshall Space Flight Center, Alabama
Nastrom GD, Belmont AD. 1978. *Geophys. Res. Lett.* 5:665–68
National Research Council. 1989. *Ozone Depletion, Greenhouse Gases, and Climate Change.* Washington, DC: Natl. Acad. 122 pp.
National Research Council. 1994. *Solar Influences on Global Change.* Washington, DC: Natl. Acad. 163 pp.
National Research Council. 1995. *A Science Strategy for Space Physics*, Space Studies Board. Washington, DC: Natl. Acad. 81 pp.
National Space Weather Program. 1995. *The Strategic Plan FCM-P30-1995*. Washington, DC/Silver Springs, MD: Off. Fed. Coord. Meteorol. Serv. Supp. Res. 18 pp.
Nesme-Ribes E, Baliunas SL, Sokoloff D. 1996. *Sci. Am.* 275(August):46–52
Nesme-Ribes E, Ferreira EN, Sadourny R, Le Truet H, Li ZX. 1993. *J. Geophys. Res.* 98: 18923–35
Newkirk G Jr. 1983. *Annu. Rev. Astron. Astrophys.* 21:429–67
Nicolet M, Swider W Jr. 1963. *Planet. Space Sci.* 11:1459–82
North GR, Kim K-Y. 1995. *J. Clim.* 8:409–17
Noyes RW, Raymond JC, Doyle JG, Kingston AE. 1985. *Astrophys. J.* 297:805–15
Paetzold HK. 1973. *Pure Appl. Geophys.* 106–108:1308–11
Peixoto JP, Oort AH. 1992. *Physics of Climate.* New York: Am. Inst. Phys. 520 pp.
Penner JE, Chang JS. 1979. *J. Geophys. Res.* 85:5523–28
Penner JE, Charlson RJ, Hales JM, Laulainen NS, Leifer R, et al. 1994. *Bull. Am. Meteorol. Soc.* 75:375–400
Pittock AB. 1978. *Rev. Geophys. Space Phys.* 16:400–20
Quiroz RS. 1979. *J. Geophys. Res.* 84:2415–20
Ramaswamy V, Schwarzkopf MD, Randel WJ. 1996. *Nature* 382:616–18
Randel WJ, Cobb JB. 1994. *J. Geophys. Res.* 99:5433–47
Ratcliffe JA. 1972. *An Introduction to the Ionosphere and Magnetosphere.* Cambridge: Cambridge Univ. Press. 256 pp.
Reeves EM. 1976. *Solar Phys.* 46:53–72
Reid G. 1991. *J. Geophys. Res.* 96:2835–44
Reid G. 1995. *Rev. Geophys. Suppl.* July:535–38
Reinsel GC, Tam W-K, Ying LH. 1994. *Geophys. Res. Lett.* 21:1007–10
Rind D, Balachandran NK. 1995. *J. Clim.* 8:2080–95
Rind D, Overpeck J. 1993. *Quat. Sci. Rev.* 12:357–74
Rind D, Peteet D, Kukla G. 1989. *J. Geophys. Res.* 94:12851–71
Rind D, Suozzo R, Balachandran NK, Prather MJ. 1990. *J. Atmos. Sci.* 47:475–94
Rishbeth H, Garriott OK. 1969. *Introduction to Ionospheric Physics.* New York; London: Academic. 331 pp.
Rishbeth H, Roble RG. 1992. *Planet. Space Sci.* 40:1011–26

Roble RG. 1976. *J. Geophys. Res.* 81:265–68

Roble RG. 1987. In *Solar Radiative Output Variations*, Workshop Proc., Nov. 9–11, Boulder, ed. P Foukal, pp. 1–25. Cambridge, MA: Cambridge Res. Instrum.

Roble RG, Emery BA. 1983. *Planet. Space Sci.* 31:597–614

Robuck A, Free MP. 1995. *J. Geophys. Res.* 100:11549–67

Rottman GJ. 1988. *Adv. Space Res.* 8(7):53–66

Salby ML, Shea DJ. 1991. *J. Geophys. Res.* 96:22579–95

Schatten KH. 1988. *Geophys. Res. Lett.* 15: 121–24

Schlesinger ME, Ramankutty N. 1992. *Nature* 360:330–33

Schwartz SE, Andreae MO. 1996. *Science* 272: 1121–22

Schwarzkopf MD, Ramaswamy V. 1993. *Geophys. Res. Lett.* 20:205–8

Solomon S, Portmann RW, Garcia RR, Thomason LW, Poole LR, McCormick MP. 1996. *J. Geophys. Res.* 101:6713–27

Sonett CP, Giampapa MS, Matthews MS, eds. 1991. *The Sun in Time.* Tucson: Univ. Ariz. Press. 990 pp.

Space Environment Services Center. 1982. *Proc. of a Workshop on Satellite Drag.* March 18–19. Space Environ. Lab., Boulder, CO.

Stevens MJ, North GR. 1996. *J. Atmos. Sci.* 53:2594–608

Stolarski RS, Bloomfield P, McPeters RD, Herman JR. 1991. *Geophys. Res. Lett.* 18:1015–18

Stuiver M, Braziunas TF. 1993. *Holocene* 3(4): 289–305

Tang F, Howard R, Adkins JM. 1984. *Solar Phys.* 91:75–86

Tobiska K. 1993. *J. Geophys. Res.* 98:18879–93

Tsuneta S, Acton L, Bruner M, Lemen J, Brown W, et al. 1991. *Solar Phys.* 136:37–67

Vallance Jones A, ed. 1993. *Environmental Effects on Spacecraft Positioning and Trajectories. Geophys. Monogr. 73.* Washington, DC: Am. Geophys. Union. 173 pp.

Vernazza JE, Avrett EH, Loeser R. 1976. *Astrophys. J. Suppl. Ser.* 30:1–60

Warren HP, Mariska JT, Lean J, Marquette W, Johannesson A. 1996. *Geophys. Res. Lett.* 23:2207–10

White OR, ed. 1977. *The Solar Output and Its Variation.* Boulder: Colo. Assoc. Univ. Press. 526 pp.

White OR, Rottman GJ, Woods TN, Knapp BG, Keil SL, et al. 1994. *J. Geophys. Res.* 99:369–72

White OR, Skumanich A, Lean J, Livingston WC, Keil SL. 1992. *Publ. Astron. Soc. Pac.* 104:1139–43

White WB, Lean J, Cayan D, Dettinger M. 1997. *J. Geophys. Res.* 102:3255–66

Wigley TM, Raper SCB. 1990. *Geophys. Res. Lett.* 17:2169–72

Willson RC. 1994. In *The Sun as a Variable Star,* ed. JM Pap, C Fröhlich, HS Hudson, SK Solanki, IAU Colloq. 143, pp. 4–10. Cambridge: Cambridge Univ. Press

Willson RC, Hudson HS. 1991. *Nature* 351:42–44

Withbroe GL. 1990. *Adv. Astronaut. Sci.* 71: 727–43

Woods TN, Prinz DK, Rottman GJ, London J, Crane PC, et al. 1996. *J. Geophys. Res.* 101:9541–69

Woods TN, Rottman G. 1996. *J. Geophys. Res.* Submitted

World Meteorological Organization. 1991. *Scientific Assessment of Ozone Depletion. Global Ozone Research and Monitoring Project—Report No. 25.* Geneva, Switzerland: World Meteorol. Org.

Wuebbles DJ, Kinnison DE, Grant KE, Lean J. 1991. *J. Geomag. Geoelectr. Supp.* 43:709–18

Zhang Q, Soon WH, Baliunas SL, Lockwood GW, Skiff BA, Radick RR. 1994. *Astrophys. J.* 427:L111–14

Annual Review of Astronomy and Astrophysics
Volume 35, 1997

CONTENTS